Research Square

Preprints are preliminary reports that have not undergone peer review.
They should not be considered conclusive, used to inform clinical practice,
or referenced by the media as validated information.

Bogong moths navigate using a light-dependent geomagnetic inclination compass

Eric Warrant

Eric.Warrant@biol.lu.se

Lund University https://orcid.org/0000-0001-7480-7016

Hui Chen

Lund University

Linnea Rosberg

Lund University

David Dreyer

Lund University

Bo Leberecht

Carl von Ossietzky Universität Oldenburg

Henrik Mouritsen

University of Oldenburg https://orcid.org/0000-0001-7082-4839

Pauline Fleischmann

Carl von Ossietzky Universität Oldenburg

Biological Sciences - Article

Keywords: migration, navigation, geomagnetic inclination compass, radical-pair mechanism, Bogong moth, Agrotis infusa

Posted Date: April 29th, 2026

DOI: https://doi.org/10.21203/rs.3.rs-9526335/v1

License: This work is licensed under a Creative Commons Attribution 4.0 International License.
Read Full License

Additional Declarations: There is **NO** Competing Interest.

Bogong moths navigate using a light-dependent geomagnetic inclination compass

Hui Chen[1], Linnea Rosberg[1], David Dreyer[1,2], Bo Leberecht[3,4], Henrik Mouritsen[3,4], Pauline N. Fleischmann[3,4*], Eric Warrant,[1,5,6*]*

1. Lund Vision Group, Department of Biology, Lund University, Sölvegatan 35, 22362 Lund, Sweden
2. Dept. Physics, Lund University, Sölvegatan 14c, 22363 Lund, Sweden
3. Institute for Biology and Environmental Sciences, Carl von Ossietzky University Oldenburg, 26129 Oldenburg, Germany
4. Research Center Neurosensory Science, Carl von Ossietzky Universität Oldenburg, 26111 Oldenburg
5. Research School of Biology, Australian National University, Canberra ACT, Australia
6. School of Engineering, University of South Australia, Adelaide, Australia

*Correspondence: hui.chen@biol.lu.se, pauline.fleischmann@uni-oldenburg.de, eric.warrant@biol.lu.se

Keywords: migration, navigation, geomagnetic inclination compass, radical-pair mechanism, Bogong moth, *Agrotis infusa*

ORCID IDs
Hui Chen: 0009-0002-1866-5169
Linnea Rosberg: 0009-0008-3433-8292
David Dreyer: 0000-0003-4344-8596
Bo Leberecht: 0000-0001-9672-1504
Henrik Mouritsen: 0000-0001-7082-4839
Pauline N. Fleischmann: 0000-0002-5051-884X
Eric Warrant: 0000-0001-7480-7016

Bogong moths (*Agrotis infusa*) migrate biannually up to 1,000 km between their breeding areas and geographically restricted aestivation sites in the Australian Alps[1,2]. These moths navigate towards their distant goal using the stars as a compass[3] but navigate correctly even when the stars are obscured by clouds[3], suggesting that their magnetic sense[4] likely harnesses the Earth's magnetic field as a compass. However, the nature of this compass, and of the magnetic sense underlying it, remain unknown. Here we show that Bogong moths, tethered in a flight arena under a full-spectrum randomised starry night sky, navigate in their inherited migratory direction using the geomagnetic field alone. If both field inclination and polarity are turned by 180°, or if inclination is turned alone, moths fly in the opposite direction. If polarity is turned alone, moths fail to turn. Furthermore, if violet-blue light (380 nm < λ < 500 nm) is removed from the illumination spectrum, or if tethered moths are exposed to weak broadband radiofrequency fields (150 kHz – 60 MHz), magnetic orientation is abolished. Our results indicate that Bogong moths use the geomagnetic field as an inclination compass for long-distance navigation at night and possess a light-dependent radical-pair-based magnetic sense[5].

The Bogong moth (*Agrotis infusa*) is an iconic Australian insect and a well-known long-distance nocturnal navigator[1-4] (Fig. 1a). During their year-long lives, individual moths undertake a long spring migration of up to 1000 km, from breeding grounds distributed all over south-eastern Australia, to a select number of geographically restricted aestivation sites in the Australian Alps[1,2] (Fig. 1b). After around 3 months of dormancy in cool alpine refuges (Fig. 1c), the same individuals return to their breeding grounds in autumn, where they reproduce and die. To make these two great seasonal journeys, Bogong moths rely on the stars as a compass to navigate in their inherited migratory direction[3]. Interestingly, when the stars are obscured by clouds, moths maintain their migratory heading[3], suggesting that the Earth's magnetic field is also likely used as a compass. The Bogong moth's previously described magnetic sense[4] only reinforces this possibility. However, the ability of the Bogong moth to use a geomagnetic compass, as well as the nature of the moth's magnetic sense itself, both remain unknown.

Here we show that Bogong moths can use the Earth's magnetic field alone as a compass to navigate in their inherited migratory direction at night, and that similar to night-migratory birds[6-8], this compass is based on the field's inclination rather than its polarity. Our results further show that again like in birds[9-15], this geomagnetic compass relies on a light-dependent radical-pair-based magnetic sense[5], possibly mediated by cryptochromes.

Bogong moths use a geomagnetic compass

During their biannual migrations, we captured southward-arriving spring migrants and northward-departing autumn migrants using a light trap located at Mt. Selwyn, approximately 70 km north-northeast of the major alpine aestivation sites in southeast New South Wales[3,4]. Moths were transferred to a purpose-built, highly ferromagnetic-free dark laboratory at our nearby field site where the moths were tethered and flown in a flight simulator arena[3,16] (details of the laboratory, the simulator design, the tethering procedures and the criteria used to select moths for analysis are provided in the Methods and Extended Data Fig. 1). This simulator continuously measured the flight headings of actively flying moths free to turn in any azimuthal direction, thus enabling the reconstruction of a "virtual flight trajectory" over a certain period

of time. The cylindrical interior wall of the flight arena was lined with blue cardboard (the "sky") and the lower third of the wall was lined with second layer of black cardboard cut to create the panoramic silhouette of a surrounding landscape (of meadows, trees, and hills). This landscape provided visual details that assisted tethered moths to control their flight.

To test whether Bogong moths possess a magnetic compass, we placed the flight simulator arena within a three-dimensional double-wound Helmholtz coil system in our laboratory. These coils allowed us to (1) rotate the azimuthal orientation of a natural geomagnetic field within the arena without altering its intensity or inclination angle, and (2) null (i.e. remove) the geomagnetic field.

Tethered moths were exposed to a full-spectrum (UV-red) randomised starry night sky (lacking directional information) that was projected at natural stellar intensity onto a flat screen placed on top of the cylindrical arena (Fig. 2a). The flights of tethered moths were recorded for 5 min. When exposed to the natural geomagnetic field and randomised stars, moths oriented in their seasonally appropriate migratory directions during two spring (2023-2024) and two autumn (2024-2025) migratory seasons. In spring, moths flew roughly southwest (mean vector direction $\alpha = 223°$, n = 122, $p = 9.1\times10^{-6}$, Fig. 2a), while in autumn, moths flew north-northeast ($\alpha = 17°$, n = 126, $p = 7.4\times10^{-5}$, Fig. 2a). Note that the spread of moth flight directions is greater than we have previously observed under natural starry skies in a nulled geomagnetic field[3] (also see Fig. 4), almost certainly due to the inherent noisiness of the magnetic sense compared to the visual sense[17]. When the azimuth of the geomagnetic field was rotated by 180° (Fig. 2b), both spring moths and autumn moths flew in almost exactly the opposite directions, turning by 191° in spring ($\alpha = 32°$, n = 128, $p = 1.5\times10^{-10}$) and by 205° in autumn ($\alpha = 222°$, n = 132, $p = 1.3\times10^{-8}$). In the absence of a geomagnetic field, but still in the presence of a randomised starry sky, moths were disoriented in both seasons (spring: n = 122; autumn: n = 124, Fig. 2c). Individual data sets from each season are provided in Extended Data Fig. 2 and full statistics in Extended Data Table 1. Moth flight directions differed significantly between spring and autumn, as well as between rotated and unrotated geomagnetic fields in each season (Watson–Wheeler tests with Bonferroni correction; Extended Data Table 1).

In summary, our behavioural results demonstrate that Bogong moths can use the Earth's magnetic field alone as a compass to navigate in their inherited migratory direction during both spring and autumn. But does this compass allow moths to find their direction using the polarity of the geomagnetic field, as observed in ants[18], or by using the field's inclination angle, as observed in birds[6-8]?

A compass based on magnetic inclination

To determine whether the magnetic compass of the Bogong moth functions as a polarity or inclination compass, the flight simulator was again positioned within a three-dimensional Helmholtz coil system in our laboratory. Three magnetic field conditions of equal intensity were established (Fig. 3): (1) natural geomagnetic field (NMF); (2) a geomagnetic field with inverted polarity but the same magnetic axis (vertical and horizontal field components were both inverted); and (3) a geomagnetic field with the same horizontal polarity as the NMF but with inverted inclination (the vertical field component alone was inverted). When spring moths were exposed to the natural magnetic field, they oriented consistently south-westward

($\alpha = 208°$, n = 77, $p = 1.1 \times 10^{-7}$; Fig. 3a). When magnetic polarity was reversed by 180° without altering the magnetic field axis and thus the inclination, moths did not respond to the polarity inversion and maintained a south-westward flight direction ($\alpha = 213°$, n = 78, $p = 5.4 \times 10^{-5}$; Fig. 3b). In contrast, when magnetic inclination was modified by only inverting the vertical component of the geomagnetic field, moths oriented northeast ($\alpha = 27°$, n = 76, $p = 5.4 \times 10^{-4}$; Fig. 3c). Collectively, these results demonstrate that Bogong moths, like birds[6-8], possess a geomagnetic inclination compass—one that distinguishes between 'poleward' (indicated by the largest possible angle between the field lines and Earth's surface) and 'equatorward' (indicated by the smallest possible angle between the field lines and Earth's surface) rather than indicating 'north' and 'south'. To investigate whether this inclination-based compass relies on a light-dependent (potentially cryptochrome-based) radical-pair mechanism, we next tested the two key predictions of the radical-pair hypothesis: that the compass requires UV or blue light and should be disrupted in the presence of broadband radiofrequency (RF) noise.

The compass requires violet-blue light

A small number of viable non-mutually exclusive hypotheses have arisen to explain how magnetic fields may be sensed[5-6,19-22]. Of these, two hypotheses have received the most attention. The first involves the presence of tiny magnetite crystals clustered within, or close to, sensory cells[23,24]. Changes in the orientation of these crystals relative to the direction of the Earth's magnetic field is thought to give rise to mechanical tensions between the magnetite crystal and the sensory cell, thereby facilitating signal transduction. This mechanism, apparently detecting the polarity of the magnetic field, has been suggested in ants[18,25], fish[26,27] and sea turtles[28], among others. The second hypothesis involves a light-dependent cryptochrome-based radical-pair mechanism[5,29-34], in which light-excited cryptochrome molecules are thought to be involved in chemical reactions that are modulated by the direction of the Earth's magnetic field. These reactions are hypothesised to trigger sensory transduction in a magnetically sensitive cell. This mechanism, able to detect the inclination but not the polarity of the magnetic field, has been suggested in several species including birds[5-8], insects[34] and sea turtles[28].

The radical-pair mechanism exhibits two distinguishing properties. Firstly, certain wavelengths and intensities of light seem necessary to allow magnetic sensation[9-11]. For example, Monarch butterflies (*Danaus plexippus*) seem to use a cryptochrome-based magnetic sense[33] that requires violet light (380-430 nm), even though the evidence for geomagnetic orientation during migration is mixed[35-37]. Secondly, according to theory[5,29,30,38], the radical-pair mechanism (and thus any magnetic sense depending on it) is disrupted by very weak broadband radio frequency (RF) noise[12-15,32-33]. We used these two properties to ask whether the magnetic sense of the Bogong moth is based on a light-dependent radical-pair mechanism.

First, we tested the light-dependency of magnetic orientation by exposing moths captured during two spring and two autumn migratory seasons (2023–2025) to natural geomagnetic fields under a projected sky of randomised stars (Extended Data Fig. 1c) in an arena lined with a panoramic scene (as in Fig. 2, Extended Data Fig. 1d,e). Experiments were again conducted in our ferromagnetic-free laboratory, but now with UV, violet and blue light removed from the stellar illumination spectrum (via a spectral blocking filter: only light of wavelength $\lambda > 500$

nm remained). Under these conditions, moths were disoriented in both seasons (Fig. 4a, Extended Data Fig. 2d), suggesting that their geomagnetic compass is light-dependent and requires light of wavelength $\lambda < 500$ nm to function.

To address the possibility that this apparent loss in magnetic orientation was instead due to moths being unable to visually control their flight in the absence of UV, violet and blue light (and thus potentially becoming disoriented), we flew spring-migratory Bogong moths in a nulled geomagnetic field under a projected natural spring starry sky (see Extended Data Fig. 1b). Under these conditions, and under full-spectrum stellar illumination, moths have previously been shown to use their stellar compass (i.e. their visual sense) to orient in their inherited migratory direction[3]. The orientation of each moth was measured during three sequential 5-minute experimental phases (Figs. 4b-d): A1, B and A2. Full-spectrum stellar illumination was provided in phases A1 and A2, but UV, violet and blue light were excluded from this spectrum during phase B. Moths maintained consistent orientation in their inherited migratory direction in all three phases (A1, Fig. 4a: $\alpha = 188°$, $R^* = 1.753$, $p = 5.2\times10^{-4}$; A2, Fig. 4c: $\alpha = 182°$, $R^* = 1.733$, $p = 6.4\times10^{-4}$; B, Fig. 4b: $\alpha = 158°$, $R^* = 1.862$, $p = 1.6\times10^{-4}$), with no significant differences between distributions (Wheeler-Watson test: W = 2.561, $df = 4$, $p = 0.634$). These results demonstrate that the disorientation we observed in the absence of UV, violet and blue light (Fig. 4a) does not arise from an inability to visually control flight. Instead, it must arise from an impaired magnetic sense. This confirms that Bogong moths possess a light-dependent geomagnetic compass mechanism.

To further investigate the light dependency of the Bogong moth geomagnetic compass, we investigated which spectral bands of illumination influence this compass. We captured moths migrating northwards during autumn[3,4] and transferred them to our outdoor site at Adaminaby. Here they experienced the natural night sky and the Earth's natural magnetic field. Moths were tested in transparent UV-transmissive Perspex flight arenas[16] (with a full view of the surrounding landscape) whose internal light spectrum was manipulated using spectral long-pass filter sheeting (Lee filters; see Extended Data Fig. 3 for details) that was placed around the outer walls of the arena, as well as on its lid and floor. A wide black disk, positioned on the shaft 3 cm above the tethered moth, blocked a direct view of the entire sky, preventing moths from using their stellar compass[3]. Four spectrally filtered arenas were designed (details in Methods and Extended Data Fig. 3b): (1) a Clear Arena (full spectrum, $\lambda > 310$ nm), (2) a UV-blocked Arena ($\lambda > 380$ nm), (3) a UV-blue-blocked Arena ($\lambda > 500$ nm) and (4) a Clear-ND Arena (full spectrum, $\lambda > 310$ nm, but reduced in intensity by ≈ 8 times due to the addition of 0.9 log unit neutral density (ND) filter sheeting). This fourth arena controlled for the possibility that disorientation was due to a decreased illumination intensity from the UV and blue blocking filters, rather than by the restricted spectrum.

We first performed two experiments (Extended Data Fig. 3c): flight orientation (1) in a Clear Arena versus a UV-blocked Arena, and (2) in a Clear Arena versus a UV-blue-blocked Arena. For each night's experiment (1 or 2), a cohort of 40 moths was divided into two groups of 20 which then underwent two experimental phases. For each phase, the two groups were tested in parallel in each of the two arenas placed 8 m apart (Extended Data Fig. 3a). After the first phase of testing, the two groups of moths were swapped between arenas for a second phase to control for possible orientation to local landmarks seen from within each arena. In both experiments (1

and 2), there were no significant differences in the orientations of the cohorts of moths flown in each arena in the two phases (Watson-Wheeler tests; Extended Data Fig. 4, Extended Data Table 2), indicating that landmarks in the landscape seen through the transparent arena walls played no role in moth orientation (as also seen in earlier studies[3]).

In Clear Arenas, moths exhibited significant orientation in their inherited migratory direction in both experiments (Experiment 1, Fig. 5a: α = 23°, n = 105, R^* = 1.841, p = 7.7×10^{-4}; Experiment 2, Fig. 5c: α = 19°, n = 122, R^* = 2.197, p = 1.0×10^{-5}), and these two mean directions were not significantly different (Watson-Wheeler tests: W = 1.915, df = 2, p = 0.384). When tested in the Clear-ND Arena (λ > 310 nm, light levels reduced ≈ 8 times), moths maintained their inherited migratory direction (Fig. 5e: α = 11°, n = 75, R^* = 1.559, p = 0.013). The same was true in a UV-blocked Arena (λ > 380 nm, Fig. 5b: α = 24°, n = 91, R^* = 1.868, p = 5.8×10^{-4}). However, when tested in the UV-blue-blocked Arena (λ > 500 nm), moths were disoriented (n = 112, Fig. 5d). Collectively, these findings indicate that violet-blue wavelengths between 380 nm and 500 nm are critical for the light-dependent magnetic compass sense of Bogong moths, even under reduced light intensity.

In summary, our results suggest that Bogong moths employ a light-dependent geomagnetic compass for long-distance navigation at night. The dependence of this compass on violet-blue light is also consistent with a magnetic sense mediated by a radical-pair mechanism (potentially cryptochrome-based). This band of wavelengths has been found necessary for magnetic orientation in other insects[34], as well as in amphibians[39] and birds[9-11], with these animals becoming disoriented in the absence of these wavelengths (e.g. when exposed only to red light) [10,11]. Although CRY1 and/or CRY2 have been indicated to mediate light-dependent magnetosensation in some insects[34,40], which (if any) of these CRYs underlies magnetic orientation in Bogong moths remains an open question.

The compass fails with RF noise exposure

To further investigate whether the Bogong moth geomagnetic compass relies on a radical-pair mechanism, we leveraged the second key prediction of the cryptochrome radical-pair hypothesis: magnetic orientation should be disrupted by very weak broadband radiofrequency (RF) noise. Autumn-caught moths were transferred to our ferromagnetic-free laboratory and again flown within a panorama-walled arena. As before, full-spectrum (UV-red) randomised stars at natural intensity were projected above the moth, and a local natural geomagnetic field was generated within the arena. The arena was encircled by a specially crafted antenna connected to a signal generator (see the Methods and Extended Data Fig. 5a,b) that produced weak broadband radiofrequency noise (range ~150 kHz to ~60 MHz; Extended Data Fig. 5c). In a natural geomagnetic field, and in the absence of RF noise, autumn migrants showed their normal inherited northward orientation (α = 18°, n = 64, R^* = 1.729, p = 6.4×10^{-4}, Fig. 6a). When the geomagnetic field was rotated by 180° (so that magnetic north points south) moths were oriented southward (α = 217°, n = 67, R^* = 2.249, p = 1.4×10^{-6}, Fig. 6c), reinforcing the results of Fig. 2. However, when weak broadband RF noise was introduced into the arena, moths became disoriented in both conditions (n = 58, Fig. 6b; n = 52, Fig. 6d). These results show that broadband RF noise disrupts the geomagnetic compass of Bogong moths, as it also

254 does in night-migratory birds[12-15,32-33], reinforcing the evidence that the magnetic sense of
255 Bogong moths relies on a radical-pair mechanism.

256 **Two compass cues for robust navigation**

257 Our results indicate that Bogong moths rely on two global compasses for robust nocturnal
258 navigation – a light-dependent radical-pair-based geomagnetic inclination compass and a stellar
259 compass[3]. This is also the case in night-migratory birds[5-15,32-33,41,42], revealing an impressive
260 example of convergent evolution in two widely separated taxa that share a similar migratory
261 behaviour. Geomagnetic and stellar compass cues enable moths to continue navigating in their
262 inherited migratory direction even when the salience of one of these cues diminishes or fails
263 (e.g. due to overcast night skies or a magnetic storm). Such robust navigation may be further
264 enhanced by the recognition of local sensory cues encountered along the journey[43]. The use of
265 global and local sensory cues at different stages of their long migration likely maximises the
266 Bogong moth's chances of arriving safely at their summer aestivation sites in the Australian
267 Alps[43]. But how these multiple sensory cues are integrated behaviourally and neurally[44] to
268 ensure robust long-distance navigation remains a fruitful avenue for future investigation.

269 **References**

270 1 Common, I. F. B. Migration and gregarious aestivation in the bogong moth, *Agrotis infusa*.
271 *Nature* **170**, 981-982 (1952).

272 2 Warrant, E. *et al.* The Australian Bogong moth *Agrotis infusa*: a long-distance nocturnal
273 navigator. *Front. Behav. Neurosci.* **10**, 77 (2016).

274 3 Dreyer, D. *et al.* Bogong moths use a stellar compass for long-distance navigation at night.
275 *Nature* **643**, 994-1000 (2025).

276 4 Dreyer, D. *et al.* The earth's magnetic field and visual landmarks steer migratory flight
277 behavior in the nocturnal Australian Bogong moth. *Curr. Biol.* **28**, 2160-2166 (2018).

278 5 Hore, P. J. & Mouritsen, H. The radical-pair mechanism of magnetoreception. *Annu. Rev.*
279 *Biophys.* **45**, 299-344 (2016).

280 6 Mouritsen, H. Long-distance navigation and magnetoreception in migratory animals.
281 *Nature* **558**, 50-59 (2018).

282 7 Wiltschko, W. & Wiltschko, R. Magnetic orientation and magnetoreception in birds and
283 other animals. *J. Comp. Physiol. A* **191**, 675-693 (2005).

284 8 Wiltschko, W. & Wiltschko, R. Magnetic compass of European robins. *Science* **176**, 62-64
285 (1972).

286 9 Wiltschko, W. & Wiltschko, R. Light-dependent magnetoreception in birds: the behaviour
287 of European robins, *Erithacus rubecula*, under monochromatic light of various
288 wavelengths and intensities. *J. Exp. Biol.* **204**, 3295-3302 (2001).

289 10 Wiltschko, W., Munro, U., Ford, H. & Wiltschko, R. Red-light disrupts magnetic
290 orientation of migratory birds. *Nature* **364**, 525-527 (1993).

291 11 Muheim, R., Backman, J. & Akesson, S. Magnetic compass orientation in European robins
292 is dependent on both wavelength and intensity of light. *J. Exp. Biol.* **205**, 3845-3856 (2002).

293 12 Hiscock, H. G., Mouritsen, H., Manolopoulos, D. E. & Hore, P. J. Disruption of magnetic
294 compass orientation in migratory birds by radiofrequency electromagnetic fields. *Biophys.*

J. **113**, 1475-1484 (2017).

13 Engels, S. *et al.* Anthropogenic electromagnetic noise disrupts magnetic compass orientation in a migratory bird. *Nature* **509**, 353-356 (2014).

14 Schwarze, S. *et al.* Weak broadband electromagnetic fields are more disruptive to magnetic compass orientation in a night-migratory songbird (*Erithacus rubecula*) than strong narrow-band fields. *Front Behav. Neurosci*. **10**, 55 (2016).

15 Ritz, T., Thalau, P., Phillips, J. B., Wiltschko, R. & Wiltschko, W. Resonance effects indicate a radical-pair mechanism for avian magnetic compass. *Nature* **429**, 177-180 (2004).

16 Dreyer, D. *et al.* A guide for using flight simulators to study the sensory basis of long-distance migration in insects. *Front. Behav. Neurosci.* **15**, 678936 (2021).

17. Johnsen, S., Lohmann, K. J. & Warrant, E. J. Animal navigation: A noisy magnetic compass? *J. Exp. Biol.* 223: jeb164921 (2020).

18 Grob, R., Wegmann, J. W., Rössler, W. & Fleischmann, P. N. Cataglyphis ants have a polarity-sensitive magnetic compass. *Curr. Biol.* **34**, 5833-5838.e5832 (2024).

19 Nordmann, G. C., Hochstoeger, T. & Keays, D. A. Magnetoreception-A sense without a receptor. *PLOS Biology* **15** (2017).

20 Johnsen, S. & Lohmann, K. J. The physics and neurobiology of magnetoreception. *Nature Reviews Neuroscience* **6**, 703-712 (2005).

21 Nimpf, S. *et al.* A putative mechanism for magnetoreception by electromagnetic induction in the pigeon inner ear. *Current Biology* **29**, 4052-4059 (2019).

22 Wiltschko, R. & Wiltschko, W. The discovery of the use of magnetic navigational information. *J. Comp. Physiol. A* **208**, 9-18 (2022).

23 Kirschvink, J. L., Walker, M. M. & Diebel, C. E. Magnetite-based magnetoreception. *Curr. Opin. Neurobiol.* **11**, 462-467 (2001).

24 Shaw, J. *et al.* Magnetic particle-mediated magnetoreception. *J. Roy. Soc. Interface* **12**, 0499 (2015).

25 Fleischmann, P. N., Grob, R., Muller, V. L., Wehner, R. & Rossler, W. The geomagnetic field is a compass cue in cataglyphis ant navigation. *Curr. Biol.* **28**, 1440-1444 e1442 (2018).

26 Fitak, R. R., Wheeler, B. R. & Johnsen, S. Effect of a magnetic pulse on orientation behavior in rainbow trout (*Oncorhynchus mykiss*). *Behav. Process.* **172** (2020).

27 Diebel, C. E., Proksch, R., Green, C. R., Neilson, P. & Walker, M. M. Magnetite defines a vertebrate magnetoreceptor. *Nature* **406**, 299-302 (2000).

28 Goforth, K. M. *et al.* Learned magnetic map cues and two mechanisms of magnetoreception in turtles. *Nature* **638**, 1015-1022 (2025).

29 Ritz, T., Adem, S. & Schulten, K. A model for photoreceptor-based magnetoreception in birds. *Biophys. J.* **78**, 707-718 (2000).

30 Xu, J. *et al.* Magnetic sensitivity of cryptochrome 4 from a migratory songbird. *Nature* **594**, 535-540 (2021).

31 Zapka, M. et al. Visual but not trigeminal mediation of magnetic compass information in a migratory bird. *Nature* **461**, 1274-1277 (2009).

32 Leberecht, B. *et al.* Upper bound for broadband radiofrequency field disruption of magnetic compass orientation in night-migratory songbirds. *PNAS* **120**, e2301153120 (2023).

33 Leberecht, B. *et al.* Broadband 75-85 MHz radiofrequency fields disrupt magnetic compass orientation in night-migratory songbirds consistent with a flavin-based radical pair magnetoreceptor. *J Comp Physiol A* **208**, 97-106 (2022).

34 Wan, G., Hayden, A. N., Iiams, S. E. & Merlin, C. Cryptochrome 1 mediates light-dependent inclination magnetosensing in monarch butterflies. *Nat. Comm.* **12**, 771 (2021).

35 Guerra, P. A., Gegear, R. J. & Reppert, S. M. A magnetic compass aids monarch butterfly migration. *Nat. Comm.* **5**, 4164 (2014).

36 Mouritsen, H. & Frost, B.J. Virtual migration in tethered flying monarch butterflies reveals their orientation mechanisms. *PNAS* **99**, 10162-10166 (2002).

37 Stalleicken, J., Mukhida, M., Labhart, T., Wehner, R., Frost, B. J. & Mouritsen, H. Do monarch butterflies use polarised skylight for orientation? *J. Exp. Biol.* **208**, 2399-2408 (2005).

38 Hiscock, H. G. *et al.* The quantum needle of the avian magnetic compass. *PNAS* **113**, 4634–4639 (2016).

39 Phillips, J. B. & Borland, S. C. Behavioural evidence for use of a light-dependent magnetoreception mechanism by a vertebrate. *Nature* **359**, 142-144 (1992).

40 Bazalova, O. *et al.* Cryptochrome 2 mediates directional magnetoreception in cockroaches. *PNAS* **113**, 1660-1665 (2016).

41 Emlen, S.T. The stellar-orientation system of a migratory bird. *Sci. Am.* **233**, 102-111 (1975).

42 Mouritsen, H. & Larsen, O.N. Migrating songbirds tested in computer-controlled Emlen funnels use stellar cues for a time-independent compass. *J. Exp. Biol.* **204**, 3855–3865 (2001).

43 Warrant, E.J. & Maleszka, R. The multisensory basis of long-distance migration in Monarch butterflies and Bogong moths - precision navigation or simply chance? *J. Exp. Biol.* **229**: jeb250957 (2025).

44 el Jundi, B. & Warrant, E. J. The sensory and neuronal mechanisms underlying long-distance migration in insects. *Curr. Opin. Neurobiol.*, in press (2026).

Figures

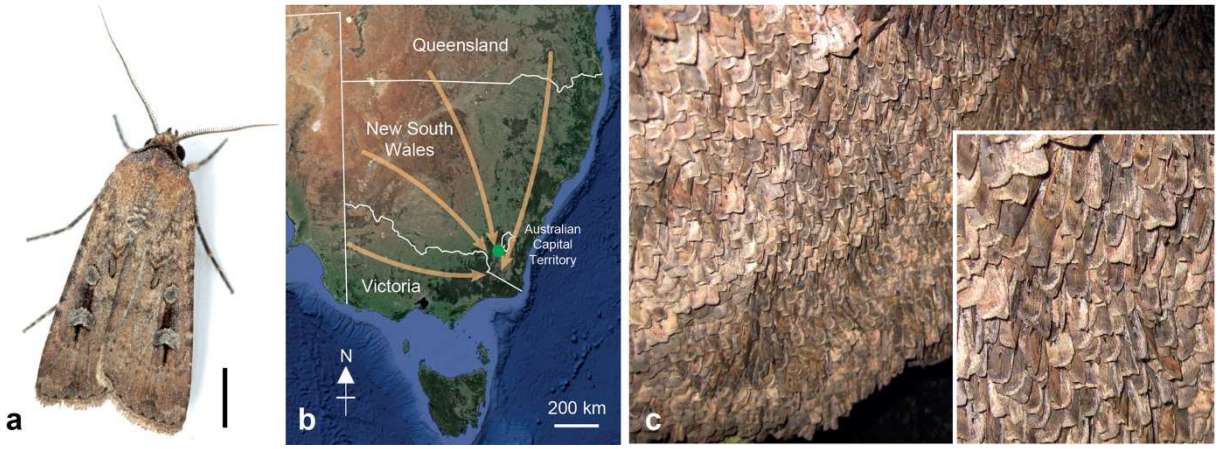


Figure 1 | The migration of the Australian Bogong moth. a. A male Bogong moth. Scale bar = 5 mm. Photo: Ajay Narendra. **b.** Likely migratory routes (*arrows*) of moths during spring to alpine regions in southeast Australia. Autumn migration occurs in the reverse directions. The *green dot* shows the location of our specialised non-magnetic lab at Adaminaby. **c.** Around 17,000 moths/m^2 aestivate on the walls of specific caves in the Australian Alps for up to 4 months before making the return migration (*inset:* detail). Photo: Eric Warrant.

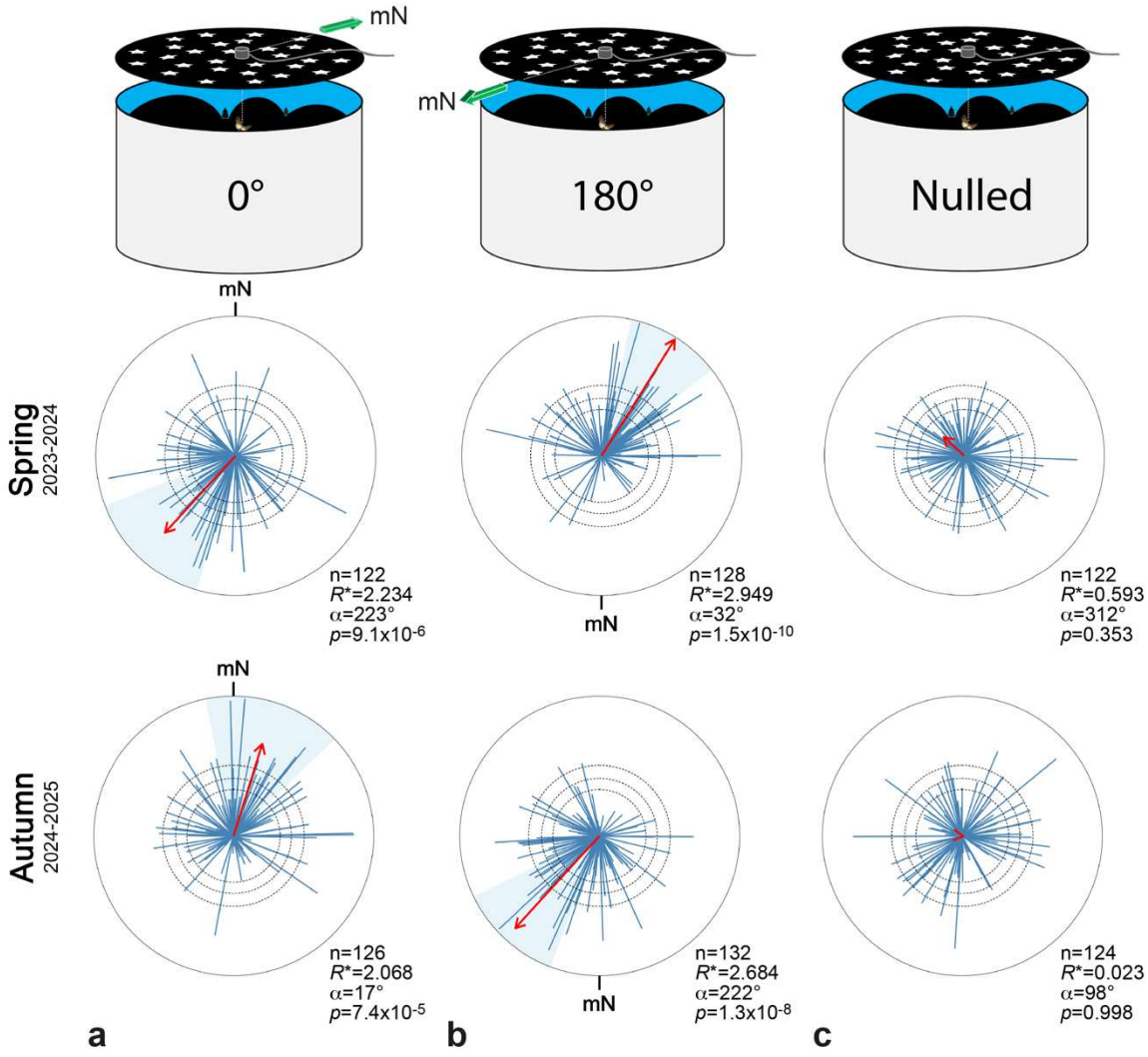


Figure 2 | Bogong moths possess a geomagnetic compass. a. Migratory moths were flown in a panorama-lined arena under a projected full-spectrum randomised starry sky and within a coil-generated natural geomagnetic field (see Extended Data Fig. 6). Moths (*light blue vectors*) flew in their inherited migratory directions in both spring ($\alpha = 223°$, n = 122 (2023 and 2024), $R^* = 2.234$, $p = 9.1\times10^{-6}$, CI_{95} = 196°-249°) and autumn ($\alpha = 17°$, n = 126 (2024 and 2025), $R^* = 2.068$, $p = 7.4\times10^{-5}$, 95% CI_{95} = 348°-46°). **b.** As for **a** except with magnetic north rotated by 180° (spring: $\alpha = 32°$, n = 128, $R^* = 2.949$, $p = 1.5\times10^{-10}$, CI_{95} = 12°-51°; autumn: $\alpha = 222°$, n = 132, $R^* = 2.684$, $p = 1.3\times10^{-8}$, CI_{95} = 200°-244°). **c.** Orientation under a randomised starry sky and in a nulled magnetic field during spring (n = 122 (2023 and 2024), $R^* = 0.593$, $p = 0.353$) and autumn (n = 124 (2024 and 2025), $R^* = 0.023$, $p = 0.998$). Each *red Mean Vector* (*MV*) in **a-c** results from weighting the mean directions and mean directedness (vector lengths) of all individual moths, as analysed by a one-sided Moore's modified Rayleigh test, with Bonferroni correction for multiple comparisons. Direction and directedness of MV given by α and R^* value, respectively. *Dashed circles:* required R^* value for statistical significance: $p < 0.05$, $p < 0.01$ and $p < 0.001$, respectively for increasing radius. *Shaded area:* 95% confidence interval (CI_{95}). mN, magnetic north.

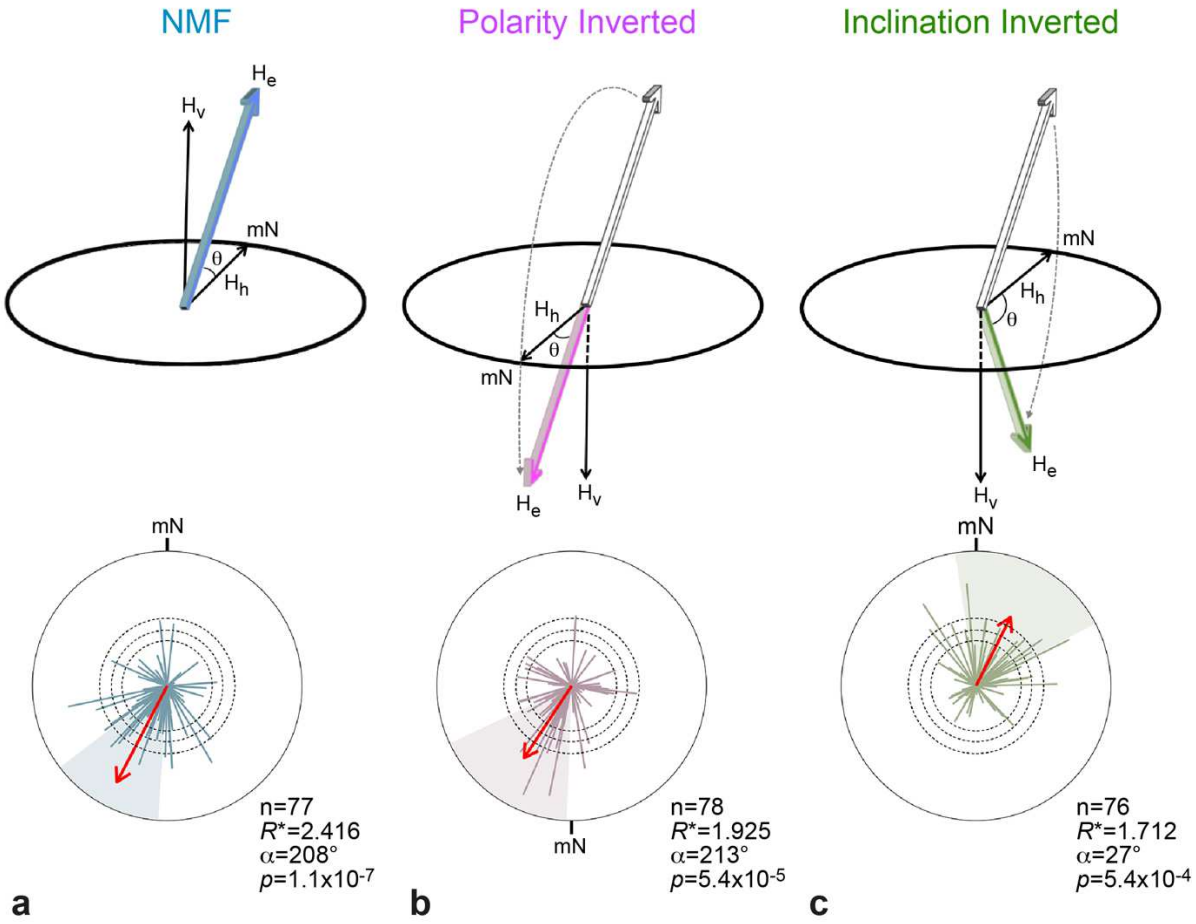


Figure 3 | Bogong moths possess a geomagnetic inclination compass. a. Spring migratory moths were flown in a panorama-lined arena under a projected full-spectrum randomised starry sky and within a coil-generated natural geomagnetic field (NMF). Moths (*light blue vectors*) flew in their inherited migratory directions ($\alpha = 208°$, n = 77, $R^* = 2.416$, $p = 1.1\times10^{-7}$, $CI_{95} = 184°\text{-}233°$). **b.** When magnetic polarity in **a** was reversed by 180° without altering inclination, moths (*light purple vectors*) persist in their inherited migratory directions ($\alpha = 213°$, n = 78, $R^* = 1.925$, $p = 5.4\times10^{-5}$, $CI_{95} = 184°\text{-}245°$). **c.** When magnetic inclination in **a** was inverted without altering polarity (via inversion of the vertical field component alone), moths oriented northeast ($\alpha = 27°$, n = 76, $R^* = 1.712$, $p = 5.4\times10^{-4}$, $CI_{95} = 351°\text{-}62°$). H_e geomagnetic field vector, H_h horizontal component of H_e, H_v vertical component of H_e, θ inclination angle, mN magnetic north. All other definitions and statistics as in Fig. 2.

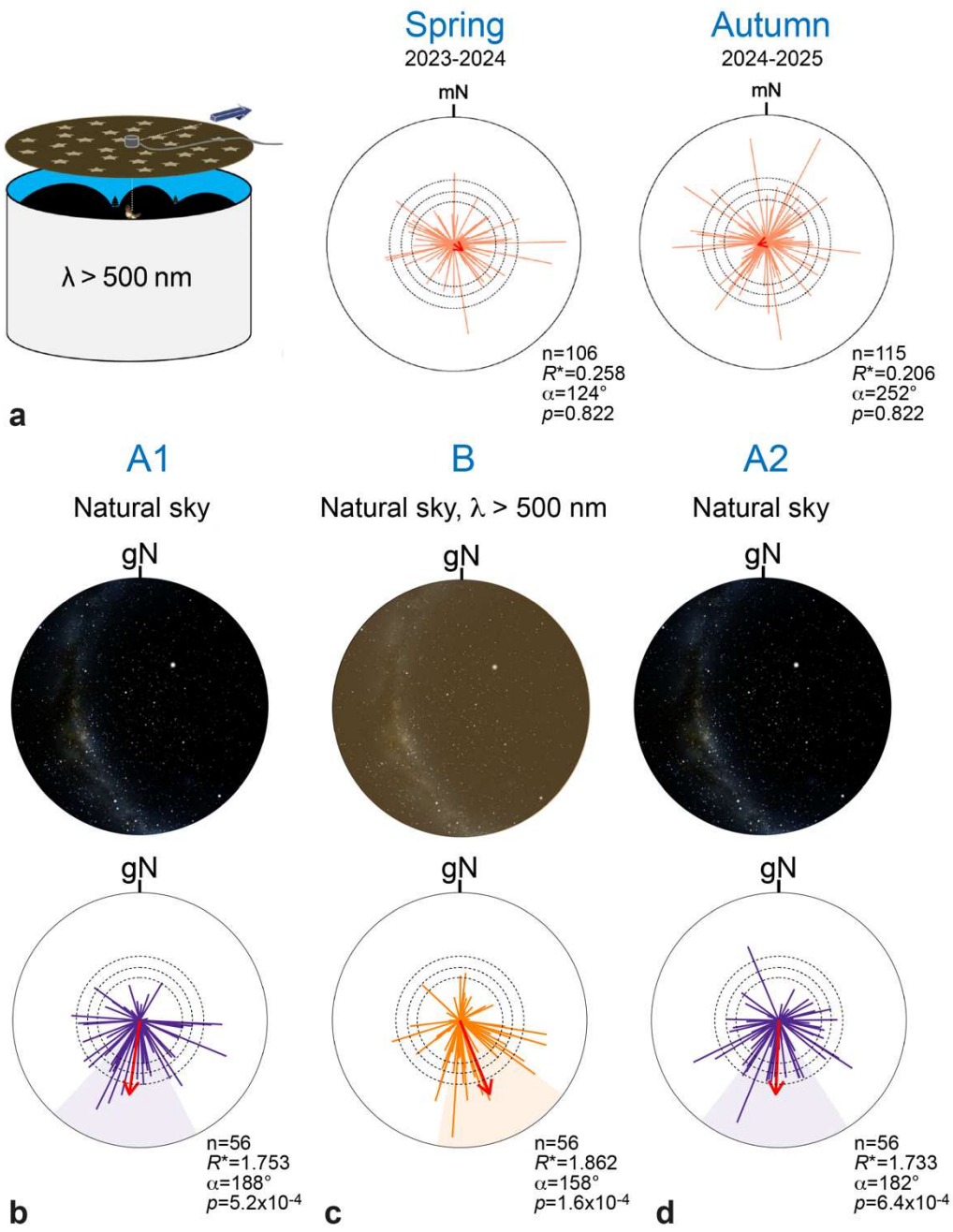


Figure 4 | The light-dependent geomagnetic compass of the Bogong moth requires light of wavelength less than 500 nm. a. With stimulus conditions the same as in Fig. 2, but with illumination restricted to λ > 500 nm, moths (*orange vectors*) were disoriented during spring (n = 106 (2023 and 2024), $R^* = 0.258$, $p = 0.822$) and autumn (n = 115 (2024 and 2025), $R^* = 0.206$, $p = 0.882$). **b,d.** Bogong moths (*purple blue vectors*) were oriented in a nulled geomagnetic field under a natural spring local starry sky with full illumination spectrum (see Extended Data Fig. 7) (**b**, Phase A1: $\alpha = 188°$, $R^* = 1.753$, $p = 5.2\times10^{-4}$, $CI_{95} = 153°\text{-}222°$; **d**, Phase A2: $\alpha = 182°$, $R^* = 1.733$, $p = 6.4\times10^{-4}$, $CI_{95} = 125°\text{-}190°$). **c.** In Phase B, moths (*orange vectors*) remained oriented in a nulled geomagnetic field under a natural starry sky lacking UV-blue light (λ > 500 nm): $\alpha = 158°$, $R^* = 1.862$, $p = 1.6\times10^{-4}$, $CI_{95} = 147°\text{-}217°$. No significant orientation differences were found among the three conditions **b-d** (Wheeler-Watson test: W = 2.561, $df = 4$, $p = 0.634$). All other definitions and statistics as in Fig. 2.

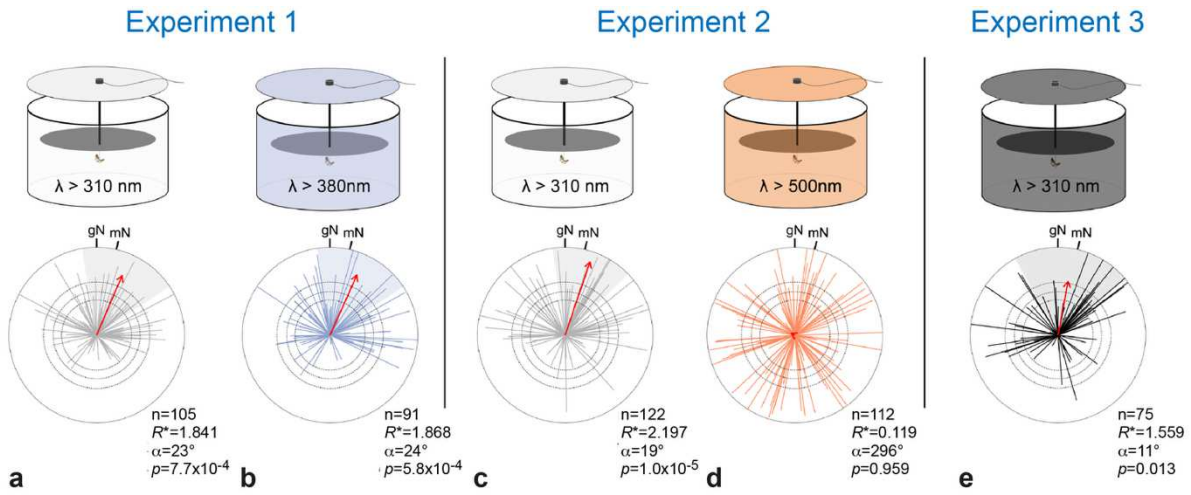


Figure 5 | The light-dependent geomagnetic compass of the Bogong moth requires violet-blue light (380 < λ < 500 nm). **a,c.** Autumn migrants tested outdoors (*grey vectors*) were oriented in a Clear Arena (passing λ > 310 nm) both in experiment 1 (**a:** $\alpha = 23°$, n = 105, $R^* = 1.841$, $p = 7.7\times10^{-4}$, $CI_{95} = 350°\text{-}56°$) and experiment 2 (**c:** $\alpha = 19°$, n = 122, $R^* = 2.197$, $p = 1.0\times10^{-5}$, $CI_{95} = 352°\text{-}46°$). **b.** Moths (*light purple vectors*) were also oriented in a UV-blocked Arena passing λ > 380 nm ($\alpha = 24°$, n = 91, $R^* = 1.868$, $p = 5.8\times10^{-4}$, $CI_{95} = 352°\text{-}56°$). **d.** Moths (*orange vectors*) were disoriented in a UV-blue-blocked Arena passing λ > 500 nm (n = 112, $R^* = 0.119$, p = 0.959). **e.** Moths (*black vectors*) were oriented (n = 75, $R^* = 1.559$, $p = 0.013$, $CI_{95} = 331°\text{-}51°$) in a Clear-ND Arena (passing λ > 310 nm, but with a reduced illumination intensity of 0.9 log units, or ≈ 8 times). All other definitions and statistics as in Fig. 2.

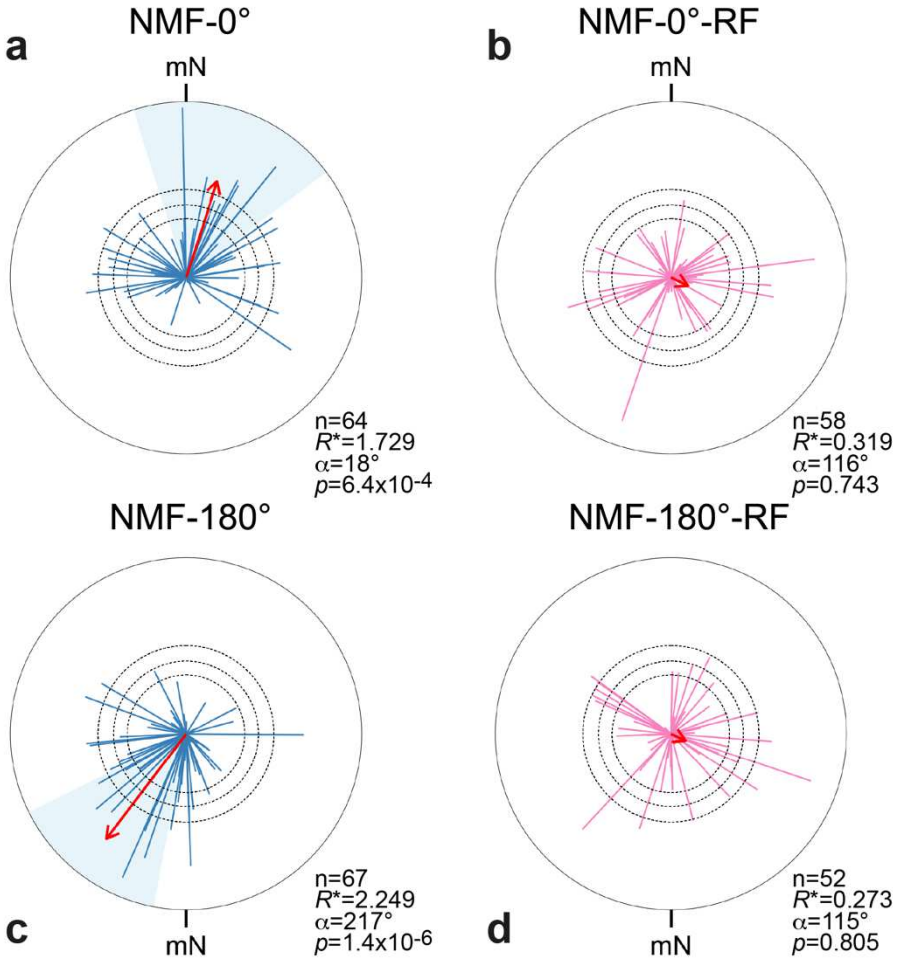


Figure 6 | Magnetic compass orientation in Bogong moths fails in the presence of broadband radiofrequency (RF) fields (~150 kHz to ~60 MHz). a, c. In a natural geomagnetic field (NMF), autumn migratory Bogong moths (*light blue vectors*) were oriented in their inherited migratory direction (**a:** natural magnetic field NMF-0°, $\alpha = 18°$, n = 64, $R^* = 1.729$, $p = 6.4\times10^{-4}$, $CI_{95} = 342°\text{-}53°$), but reversed this direction when the magnetic field was rotated by 180° (**c:** NMF-180°, $\alpha = 217°$, n = 67, $R^* = 2.249$, $p = 1.4\times10^{-6}$, $CI_{95} = 191°\text{-}243°$). **b, d.** In the presence of radiofrequency fields, moths (*pink vectors*) were disoriented irrespective of the rotation of the geomagnetic field (**b:** n = 58, $R^* = 0.319$, $p = 0.743$; **d:** n = 52, $R^* = 0.273$, $p = 0.805$). All other definitions and statistics as in Fig. 2.

Extended Methods

Capture and care of moths

Bogong moths (*Agrotis infusa*) of both sexes were captured in the wild during their autumn migration (2024-2025, Austral autumn) and spring migration (2023-2025, Austral spring), using either a Lepi LED light (www.gunnarbrehm.de) and/or a vertical beam search light (model GT175, Ammon Luminaire Company, Shanghai, China), positioned in front of a white sheet suspended between two trees. All moths were captured near Thredbo (Dead Horse Gap, southeast New South Wales (NSW), Australia: 36.524°S, 148.260°E, elevation 1580 m) and near the Mt. Selwyn Snowfields (southeast NSW, Australia: 35.914°S, 148.444°E, elevation 1600 m). Each captured moth was placed in its own small plastic container to isolate it from other moths. Upon capture, the moths were transported to the testing site at the property *Glenhare*, near Adaminaby, NSW (36.040°S, 148.864°E, elevation 1250 m). Moths were fed a 20% honey water solution every other day and housed in a cool, sheltered environment with natural photoperiod conditions.

Attachment of tethering stalks on moths

To attach tethering stalks (thin non-magnetic tungsten rods), the scales on the moth's dorsal thorax were carefully removed using a brush. The end of the tungsten stalk was bent with needle-nosed pliers to create a small circular footplate for connection to the thorax. The stalk was affixed to the moth's dorsal thorax using contact cement (Impact adhesive, EVO-STIK, UK), while the moth was gently restrained by a weighted-down plastic mesh to ensure stability. Following stalk attachment (Extended Data Fig. 1f), each moth was transferred to a ventilated clear UV-transmissive Perspex container. Shortly before sunset (approximately 1 hour before), containers were positioned on elevated rock formations to afford unobstructed views of the western sky, enabling observation of the setting sun and skylight polarisation patterns—cues hypothesised to calibrate compass mechanisms[45,46].

Apparatus for controlled behavioural experiments in the lab

All of the controlled behavioural experiments were performed in an isolated dark room with extremely low background levels of radiofrequency disturbances in our purpose-built, highly ferromagnetic-free, laboratory located at the rural property *Glenhare*, near Adaminaby[3] (built on a concrete slab reinforced with fiberglass and constructed entirely from non-magnetic materials). Captured migratory Bogong moths were tethered and flown in our modified Mouritsen-Frost flight simulator[3,16,36] within a double-wound 3D Helmholtz coil system to investigate whether moths respond to changes in a natural geomagnetic field (Extended Data Fig. 1a). All electrical grounds in the laboratory were connected in a single-point (star) configuration to minimise electrical noise, with the single point consisting of a metal rod. The experimental apparatus had its own dedicated earth separated from the mains earth (through a 6-mm thick, 30-mm wide and 12-m long copper strap dug into the ground below the concrete slab). The arena consisted of a cylindrical Perspex cylinder lined with a panoramic black cardboard silhouette of a simulated landscape (including trees, grass, and hill peaks) set against a blue cardboard “sky” backdrop (Extended Data Fig. 1d,e). A UV-transmissive Perspex lid

(diameter, 50 cm; thickness, 0.5 cm), with a layer of UV-transmissive diffusing paper (Lee Filters 251, 1/4 white diffuser), was placed on top of the arena and used for dorsal projection of celestial stimuli (see below). A customized optical encoder[45] was mounted at the centre of the lid. This encoder held a carbon fibre rod (length,15 mm; diameter, 1 mm) that extended downwards inside the arena. The tungsten tether was connected to the end of this rod, thus connecting the moth to the encoder. This encoder allowed tethered moths to rotate freely (0-360°) in the horizontal plane and to continuously record their flight heading directions (5 samples per second, angular resolution 0.9°) via customised recording software (Flash Flight Simulator Data Acquisition System, written by H.C.[3,48]). The recorded data therefore permitted us to reconstruct the moth's virtual flight path for a specified period of time under different stimulation conditions. In addition, a very dim moving pattern of optic flow was projected from below, via a 45° mirror, onto a screen (Lee Filter 251 1/4 white diffusing paper) placed beneath the arena to simulate a moving view of the ground below the flying moth[3,4,47]. The direction of the optic flow was instantaneously coupled via feedback to the moth's flight heading using custom software[3,4,47] (H.C.) so that the optic flow always moved from head to tail below the moth (Extended Data Fig. 1g).

The three-axis Helmholtz coil system, custom built in aluminium and copper (University of Oldenburg workshop; outer coil diameters: X: 1245 mm, Y: 1300 mm, Z: 700 mm), manipulated the magnetic field around the experimental moth. The coil system was powered by three constant-current power supplies (Kepco, BOP 50-2M) and the current running through the coil systems was controlled through High-Speed USB Carriers (USB-9162, National Instruments) and custom-written codes in MATLAB (Mathworks, Natick, MA). Before each experimental session, Meda FVM-400 magnetometer measurements ensured that the magnetic field was identical to the software settings (Extended Data Fig. 6).

Stimulation with starry skies

In the lab, a natural moonless starry austral night sky was projected onto the arena lid using a downward-pointing projector (LED projector ASUS S1 Mobile). The projector was mounted sufficiently high above the arena to provide clear and correctly sized dorsal images of the night sky. To avoid unwanted stray light, each projector was housed in a custom-built 3D-printed plastic box featuring an opening in front of the lens and ventilation slits above the projector. The free software Stellarium[48] was used to generate a celestial image simulating the moonless starry night sky over Canberra (approximately 80 km from Adaminaby in a straight-line) at 21:30 on the night of 22 October 2022 (Southern hemisphere spring 2022, Extended Data Fig. 1b). In addition, to prevent Bogong moths from using their stellar compass[3] for orientation during geomagnetic orientation experiments, a featureless starry sky of randomised stars[3] (Extended Data Fig. 1c) was projected. These images were projected onto the circular screen created by the lid of the arena, with the projected sky's dimensions matched to the screen size. As the projectors did not emit UV light, we installed a custom-made LED-ring (built by T. McIntyre, University of South Australia; diameter, 120 mm; inner diameter, 50 mm) featuring eight UV LEDs (LED370E Ultra Bright Deep Violet LED, Thorlabs) centred around the front lens of the projector. The brightness of the LED-ring was reduced to quasi-natural levels by neutral density filters (see below) and custom-written software in MATLAB (MathWorks, Natick, MA).

To manipulate the intensity and spectral composition of light entering the flight arena (Extended Data Fig. 7), we employed filter sheets (Lee Filters, USA) placed in front of the projector lens. Neutral Density (ND) filters (Lee Filters 210, ND 0.6 log units, transmitting $\lambda > 310$ nm) were used to attenuate light intensity uniformly across all wavelengths, preserving spectral integrity. To lower illumination intensity to natural starlight levels, 6 layers of 0.6 ND filter were placed in front of the projector lens. To block the UV-violet-blue part of this illumination spectrum, and to maintain approximately the same starlight illumination intensity, 1 layer of Egg Yolk Yellow long-pass filter (Lee Filters 768, $\lambda > 500$ nm) and 5 layers of 0.6 ND filter (Lee Filters 210) were placed in front of the projector lens. Upward illumination intensity and spectrum measurements of the projected starry night sky using these filter combinations were made from within the arena using an Ocean Optics QE65PRO Spectrometer (Ocean Optics) located underneath the projection screen at the position of the moth (Extended Data Fig. 7)[3].

Generation and measurement of radiofrequency fields

Radiofrequency fields (RF fields) were produced by a customised antenna and a noise generator (RIGOL, DG 1022, China) operating in noise mode. An output intensity of 2.5 V_{pp} (Volts peak-to-peak) was selected for our experiments (see Extended Data Fig. 5). The produced RF field intensities lay within the range of RF field intensities and broadband frequencies previously shown to disrupt magnetic compass orientation in birds[12-15] (see Extended Data Table 3). A custom-constructed ring-shaped antenna with an inner diameter of ~51 cm was made from a coaxial cable (RG58C/U MIL-C-17, BNC connector, Germany), precisely designed to fit over the exterior wall of our flight simulator arena. In brief, a 180 cm long coaxial cable with a BNC connector at one end was used. The braided shield at the opposite (cut) end was stripped to expose the central conductor. After determining the circumference to fit the arena (approximately 160 cm), the plastic sheath was removed over a 5 cm length of cable at a point 20 cm from the BNC connector end, exposing the braided shield (Extended Data Fig. 5a). The central conductor was then connected to this exposed shield to form a closed loop. The 2.5 V_{pp} of noise-mode signal was selected and then transmitted through a 5-meter-long coaxial cable (BNC connector) from the control room to the antenna (now fitted over the arena) to generate broadband noise in the ~150 kHz to ~60 MHz range (Extended Data Fig. 5c; Extended Data Table 3). The noise generator was used in 'RF OFF' mode and only switched to 'RF ON' mode for the experiments or during measurements. To calibrate the intensity of the RF noise, measurements of the generated radiofrequency fields were made at the University of Oldenburg (Germany) with a Signal Analyser (Rhode and Schwarz, FSV3004 Signal and Spectrum Analyser (10 Hz – 4 GHz), Germany) in an RF-shielded experimental chamber[14,32,33,49] using a calibrated active loop antenna (Schwarzbeck Mess-Elektronik, HFS 1546, 150 kHz–400 MHz, Germany). This antenna was connected to the FSV3004 signal analyser through the wall of the chamber via a coaxial cable with N-connectors located on the outside of the chamber. RF fields were measured for the duration of one experimental test round (5 min). For comparison to other studies that explored the effects of broadband RF fields on the orientation behaviour of animals[13,14,32,33,49], '*average*' and '*maxhold*' measurements were recorded. As described in Ref. 49, for *maxhold* measurements the detector was set to '*Maxpeak*', while for *average* measurements the detector was set to '*RMS*' (root-mean-square). The values of *maxhold* and *average* broadband RF density ($\overline{b^{\max}}$, $\overline{b}$) and intensity (B_{rms}^{max}, B_{rms}) were calculated using Equations 2.1 and 2.3 in Ref. 49 for consistency and comparability (see Extended Data Table

3). Notably, the 'RF OFF' mode (stand-by mode) provided similar measurements of density and intensity to measurements obtained with the generator set to the lowest possible output (0.004 V_{pp}) or turned off (Extended Data Fig. 5c; Extended Data Table 3).

Apparatus for behavioural experiments under an open sky in a natural landscape

Two non-magnetic Mouritsen-Frost flight simulators (the same type used in the laboratory) were placed on a hilltop at *Glenhare* and used to record the heading directions of tethered migratory Bogong moths experiencing the full local surrounding landscape in different light-filtered arenas (Extended Data Fig. 3C). Four flight simulator arenas were constructed from transparent UV-transmissive Perspex cylinders and lids (diameter, 50 cm; height, 35 cm), each fully enclosed (sides, lid and bottom) by distinct filter combinations: (1) a Clear Arena (1 layer of Lee filter 130, $\lambda > 310$nm), (2) a UV-blocking Arena (2 layers of Lee filter 226, $\lambda > 380$nm), (3) a UV-Blue-blocking Arena (2 layers of Lee filter 226 and 1 layer of Lee filter 768, $\lambda > 500$ nm), and (4) a Clear-ND Arena (1 layer of Lee filter 130 and 1 layer of 0.9 ND Lee filter 211, $\lambda > 310$nm). A tethered moth was connected to an optical encoder mounted at the centre of the lid (as described above). To prevent Bogong moths – known to employ a stellar compass[3] – from accessing sky cues, a 30 cm diameter black cardboard disk was positioned 3 cm above the tethered test moth, completely blocking its visual access to celestial cues. We ran two flight simulators in parallel on each night. These were placed on each of two aluminium tables with clear UV-transmissive Perspex tops, and these were placed 8 metres apart. The two flight simulators were controlled from computers that were operated from within a black light-tight cubical tent that was placed 10 m away from the two arenas (Extended Data Fig. 3a). The tent was therefore a landscape feature (among others) that the moths could potentially see from different directions during their tethered flights. Thus, in the experiments described below, each cohort of moths was run in both arenas to control for any possible effects of differences in visual landmarks seen from each arena.

Behavioural procedures

Indoor behavioural procedures

For tethering within the panorama-walled arena, procedures were conducted under dim red light to maintain the moth's dark-adapted visual state. Stalked Bogong moths were secured to the encoder base with a thin rubber band, and their orientation was manually aligned to Magnetic North (mN) and set as 0° in the software (i.e. 0° = mN). The optical encoder, controlled via custom software, recorded the moth's flight heading under the projected night sky. Data were sampled at 5 Hz with a 0.9° horizontal angular resolution. Each moth was tested for exactly 5 minutes per stimulus condition and the resulting virtual flight trajectory was constructed from the sampled data.

Moths chosen for analysis had to meet three *ante hoc criteria*, two prior to the experiment and one during the experiment: (1) the tethering stalk had to be perfectly vertical, (2) wing flapping had to be vigorous with a large and equal amplitude for both wings, indicating that the contact cement had not interfered with the wings, and (3) the moth had to fly continuously for the full 5 minutes. If a moth stopped flying, the arena was gently tapped to stimulate continued flight. A moth that stopped flying four times was rejected, and the recording aborted.

Outdoor behavioural procedures

The same behavioural methodologies and inclusion criteria used in indoor experiments were applied outdoors. These field experiments aimed to characterise migratory behaviour in Bogong moths experiencing the real geomagnetic field and local landscape cues – specifically open grasslands, trees, and rolling hills – from within light-filtered arenas. Experiments were performed under clear starry skies or partly overcast conditions during autumn 2025 (over 10 nights during early and late April), as well as at two times of night, to test whether the migratory orientations of moths were affected by the spectrum of light.

Each night, we conducted experiments with roughly 40 Bogong moths, testing all moths in each of two arenas across two experimental phases. We used a within-subject counterbalanced design where each moth underwent orientation measurements in both phases (i.e. in each of both arenas) to control for individual variation (Extended Data Fig. 3c). The study comprised two main experiments (experiments 1 and 2) and an intensity control (experiment 3). In experiment 1, where we blocked UV light, we simultaneously compared two cohorts of roughly 20 moths. In Phase 1 of the experiment, one cohort was flown in the Clear Arena (1 layer of Lee 130, $\lambda > 310$ nm), and one in the UV-blocked Arena (2 layers of Lee 226, $\lambda > 380$ nm). In Phase 2 of the experiment, the cohorts were then swapped to the other arena and the experiment repeated (Extended Data Fig. 3c). In experiment 2, where we blocked UV, violet and blue light, we again simultaneously compared two cohorts of roughly 20 moths in Phase 1 and swapped them to the other arena for Phase 2 (Extended Data Fig. 3c). This time the two arenas were the Clear Arena and a UV-Blue blocked Arena (2 layers Lee 226 + 1 layer Lee 768, $\lambda > 500$ nm). Finally, in experiment 3, we controlled for the possibility that any observed disorientation in experiments 1 and 2 was not simply caused by a reduction in illumination intensity arising from the UV and blue blocking filters, rather than by the reduced spectrum itself. To do this, all 40 moths were flown in a Clear-ND Arena (1 layer Lee 130 + 1 layer Lee 211 0.9 neutral density, $\lambda > 310$ nm,), whose internal intensity was reduced to a level similar to the reduction caused by the UV and UV-blue spectral filters. In all experiments, the instantaneous orientations of moths were recorded in the same way as for indoor experiments (see above). Between earlier and later experiments, tethered moths were kept isolated and in the dark in a suitcase that was warmed with hot water bottles.

Irradiances and filter transmission characteristics were again measured (Extended Data Fig. 3b) using a spectrophotometer (Ocean Optics, QE65PRO, USA). The spectral transmission of each arena was measured at the normal location of the tethered moth under natural stellar illumination.

Data analysis

The instantaneous heading directions (and the virtual trajectory) of each tethered flying moth were saved as a text file. Circular plot vectors, representing each moth's mean orientation (α) and flight path directedness (r), were calculated via the classic Rayleigh test. Normality of r values was assessed using the Shapiro-Wilk test, with parametric T-tests or non-parametric Wilcoxon/Kruskal-Wallis tests used for group comparisons based on normality results. Flight paths were visualized in R (version 4.4.3, https://www.r-project.org/, accessed 28 February 2025), and mean orientation vectors were computed for each trajectory. To leverage both mean direction (α) and directedness (r) derived from flight trajectories, we applied a one-sided

Moore's Modified Rayleigh Test (MMRT) with Bonferroni correction for multiple comparisons using custom R scripts (developed by H.C., adapted from Ref. 50)[47,50,51]. The MMRT-derived R^* value quantifies population-level directedness and orientation, indicating whether the flight directions of a population of tested moths deviated significantly from random. The exact MMRT-derived p-value was calculated by Moore's formula[4,49] (equation 3.3 in reference 51). For comparing flight direction distributions across conditions (e.g. 0° or 180° rotated magnetic fields, and different light-filtered conditions), we used the Watson-Wheeler test with Bonferroni correction in R to assess significant differences in circular distributions.

Statistics and reproducibility

Behavioural data obtained under open natural skies were obtained in independent experiments over successive nights (with new moths used each night). Behavioural data obtained in the lab under projected starry skies generated using Stellarium were obtained in independent experiments run over several nights with each night's cohort of moths used only once. Thus, all these experiments deal with biological replicates. Sample sizes were based on the availability of moths, with at least 50 moths (and as many as 130) being used for each experiment. Experiments were conducted without blinding and without a specific randomisation protocol (apart from the random selection of moths used as replicates).

References

45 Cochran, W. W., Mouritsen, H. & Wikelski, M. Migrating songbirds recalibrate their magnetic compass daily from twilight cues. *Science* **304**, 405-408 (2004).

46 Muheim, R., Phillips, J. B. & Akesson, S. Polarized light cues underlie compass calibration in migratory songbirds. *Science* **313**, 837-839 (2006).

47 Chen, H. *et al.* Adaptive migratory orientation of an invasive pest on a new continent. *iScience* **26**, 108281 (2023).

48 Zotti, G., Hoffman, S.M., Wolf, A., Chéreau, F. & Chéreau, G. The simulated sky: Stellarium for cultural astronomy research. *J. Skyscape Archeol.* **6**, 221-258 (2021).

49 Kobylkov, D. *et al.* Electromagnetic 0.1-100 kHz noise does not disrupt orientation in a night-migrating songbird implying a spin coherence lifetime of less than 10 micros. *J. Roy. Soc. Interface* **16**, 20190716 (2019).

50 Massy, R. *et al.* Hoverflies use a time-compensated sun compass to orientate during autumn migration. *Proc Biol Sci* **288**, 20211805 (2021).

51 Moore, B. R. A modification of the Rayleigh test for vector data. *Biometrika* **67**, 175-180 (1980).

Data availability

The raw data supporting the findings of Figs. 2-6 and Extended Data Figs. 2 and 4 are available at Figshare (https://doi.org/10.6084/m9.figshare.29401010.v6). Source data are provided with this paper.

714

715 **Code availability**

716 The R code for the Moore Modified Rayleigh Test (used to analyse circular raw data) is
717 available at the above Figshare site. Any additional information required to reanalyse the data
718 reported in this paper is available from the corresponding authors upon request
719 (hui.chen@biol.lu.se, eric.warrant@biol.lu.se).

720 **Author contributions.** H.C., P.N.F. and E.W. conceived the project. Preliminary experiments
721 conducted by E.W., H.M. and D.D. informed the current experimental design. H.C., D.D.,
722 H.M., P.N.F. and E.W. provided crucial logistical, experimental and intellectual input. All
723 authors were involved in the experimental design, and the design and manufacture of laboratory
724 and experimental apparatus. H.C., P.N.F., L.R., B.L. and E.W. performed the experiments. H.C.
725 calibrated the magnetic stimulation apparatus and D.D. and H.C. wrote the MATLAB scripts
726 to control it. H.C., B.L. and E.W. analysed the results. H.C. and E.W. made the figures and
727 wrote the initial version of the manuscript. All authors made substantial contributions to the
728 final version.

729 **Competing interests.** The authors declare no competing interests.

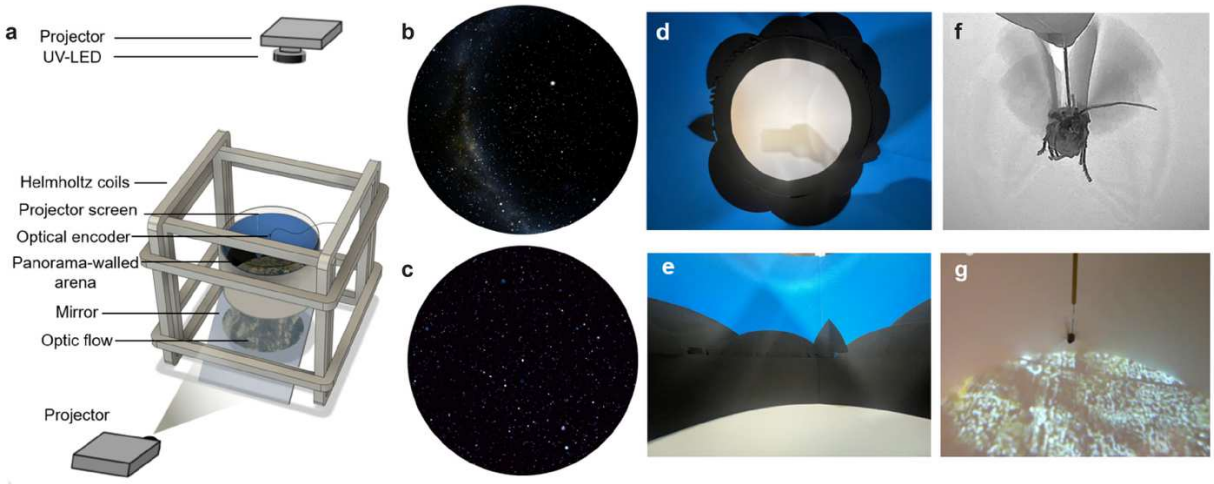
730 **Acknowledgements.** The authors are very grateful to the workshop staff at the University of
731 Oldenburg, and Lars Fredriksson at the Department of Biology in Lund, for manufacturing
732 much of the experimental apparatus. We are also grateful to Anna Honkanen, Daniel Gutierrez,
733 and Nina Griggs for help in the field, and Ajay Narendra, Macquarie University, Sydney, for
734 the photograph of the Bogong moth shown in Fig. 1A. We are also immensely grateful to Alison
735 Hastie for logistical support in Canberra and to Tim Greville, Thom Khan and the staff of the
736 NSW National Parks and Wildlife office in Jindabyne for their assistance in the Kosciuszko
737 National Park. We also wish to thank Ken Green, who contributed detailed knowledge of
738 Bogong moth ecology and aestivation sites and provided critical logistical support in the
739 Australian Alps. We are also grateful to Jingjing Xu for pilot experiments that contributed to
740 the development of the current experimental design. H.C. is supported by a postdoctoral
741 fellowship from the Wenner-Gren Foundation, Sweden, for which we are also very thankful.
742 The authors are indebted to the European Research Council (Advanced Grants Magnetic Moth~~,~~
743 (number 741298) and Incredible Journeys (number 101199455) to E.W., and the Synergy Grant
744 "Quantum Birds" (number 810002) to H.M.), the US Air Force Office of Scientific Research
745 (Grant number FA9550-14-1-0242 to E.W.), the Australian Department of Defence (Defence
746 Science and Technology Group to E.W), the Royal Physiographic Society of Lund (to E.W.),
747 the Swedish Research Council (Vetenskapsrådet, Grant number 2021-04917 to E.W.), the
748 German Research Council (Deutsche Forschungsgemeinschaft, grant number 395940726, SFB
749 1372 'Magnetoreception and navigation in vertebrates' to H.M., the Cluster of Excellence
750 "NaviSense", grant number 533653176, to H.M, P.N.F. and E.W., and the "ExzellenzStärken"
751 program of the Ministry of Science and Culture of Lower Saxony for their support of the
752 application for the Cluster of excellence "NaviSense". P.N.F. acknowledges the support of The
753 Company of Biologists for a Research Partnership Kickstart Travel Grant (JEB-KS12), and the
754 International Society for Neuroethology for the 2024 Konishi Neuroethology Research Award.
755 The research was performed under a Scientific License issued by the New South Wales National
756 Parks and Wildlife Service (no. SL100806) and took place on the traditional lands of the

757 Walgalu and Ngarigo peoples, to whose elders – past, present and future – the authors pay their
758 respect.

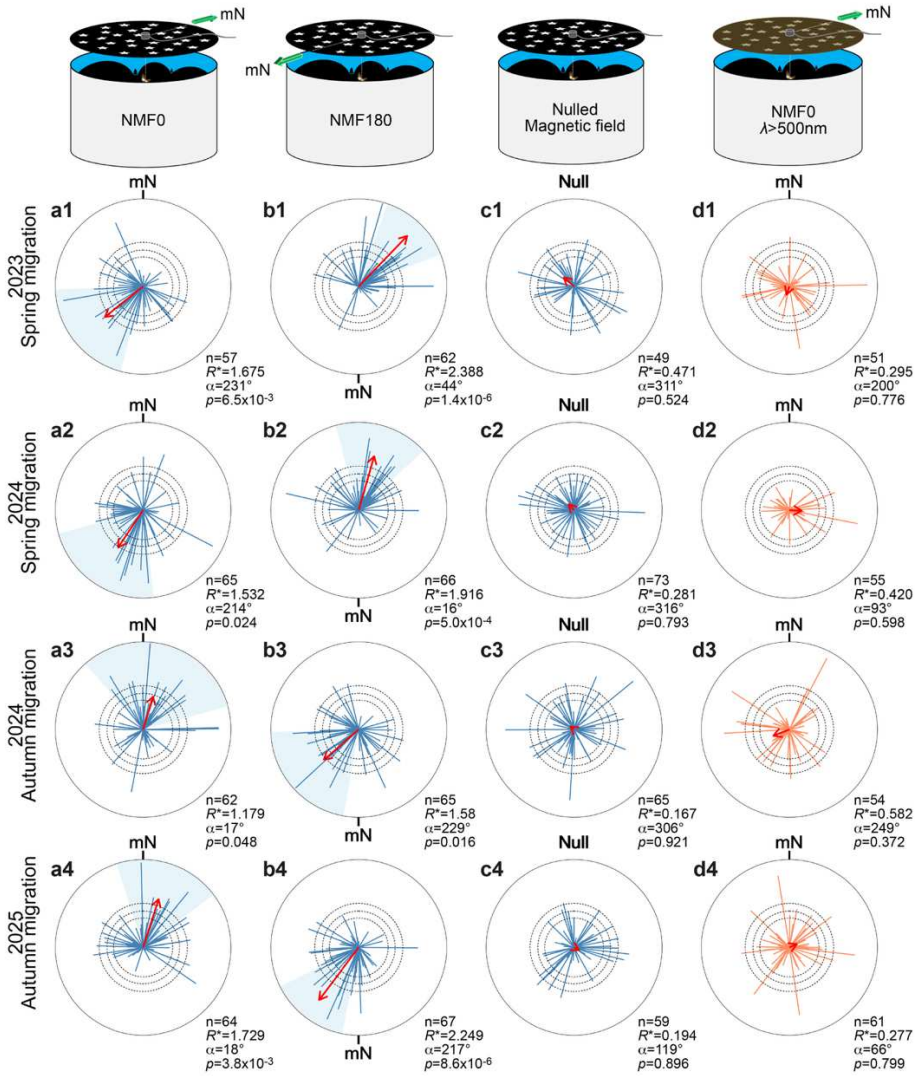
Extended Data Figures and Tables

Bogong moths navigate using a light-dependent geomagnetic inclination compass

Hui Chen, Linnea Rosberg, David Dreyer, Bo Leberecht, Henrik Mouritsen, Pauline Fleischmann, Eric Warrant



Extended Data Figure 1. **Methods for studying long-range navigation in migratory Bogong moths. a.** A diagram illustrating our non-magnetic behavioural rig for monitoring trajectories of tethered flying moths. The panorama-walled flight arena, enclosed within three-dimensional Helmholtz coils (coil outer dimensions: X: 1245 mm, Y: 1300 mm, Z: 700 mm), receives dorsal projections of a starry night sky (generated using Stellarium) on a UV-transparent Perspex circular lid topped with a UV-transmissive diffuser (Lee Filter 251, 1/4 white). This lid was placed on top of the arena and optic flow was ventrally projected onto a similarly constructed screen installed below the moth, under the arena. An optical encoder, mounted at the centre of the lid, and connected to the moth via a non-magnetic tungsten rod (**g**), records instantaneous flight headings every 200 ms. The ventral optic flow is synchronised via feedback with the moth's real-time heading using *Mapflow.exe* software, ensuring that flow direction is always nose-to-tail irrespective of the moth's heading. **b.** The projected natural starry sky at 21:30 on 15 October 2022 during the Bogong moth's southward spring migration. **c.** The projected randomised starry sky. Top-view (**d**) and moth's-eye view (**e**) of the panoramic "landscape" scene within the arena. **f.** A flying moth with a tungsten stalk seen from the front (wing flapping envelope visible). **g.** The optic flow projected beneath the moth (shown at much greater intensity than used in experiments, for the sake of visibility).

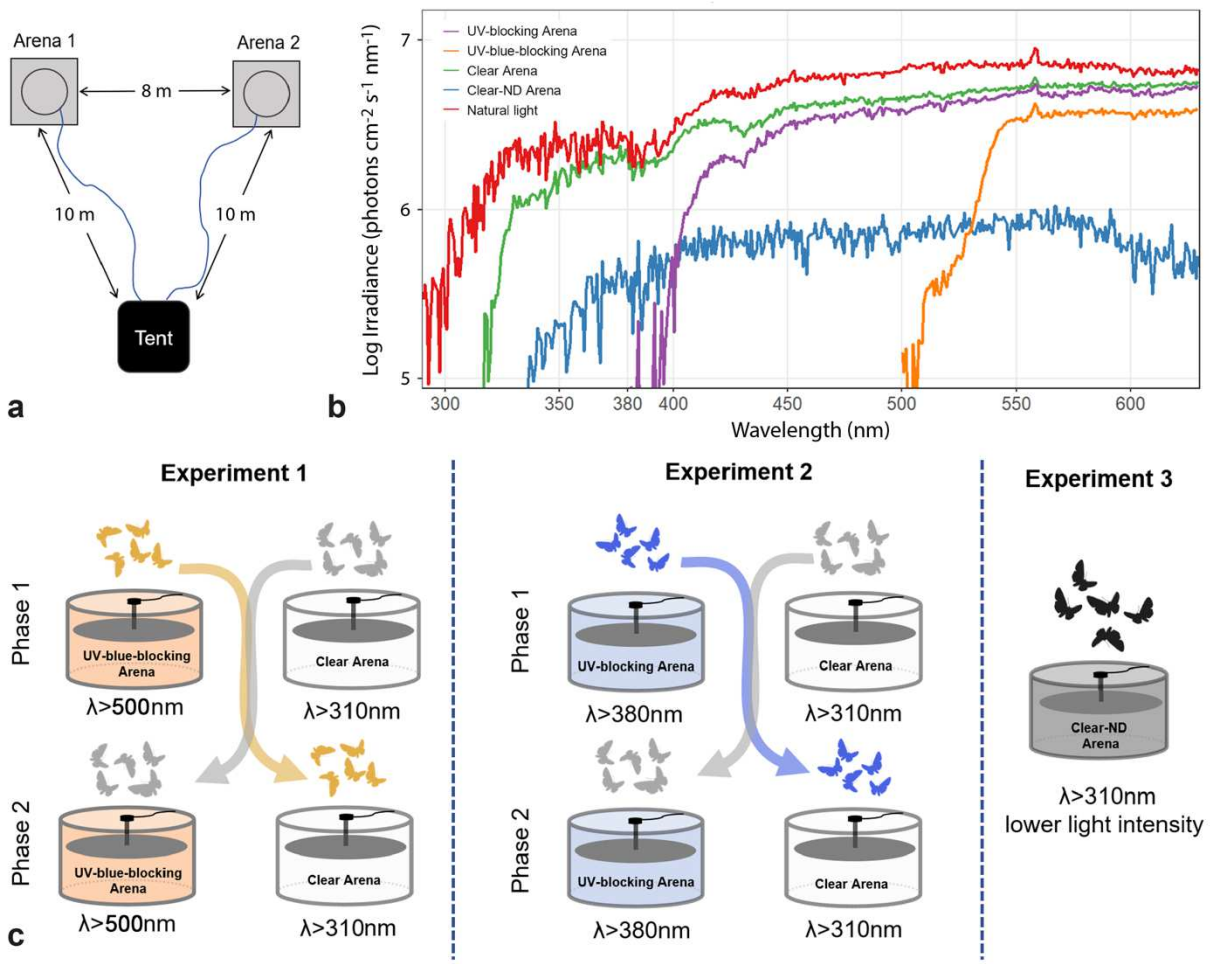


Extended Data Figure 2. **The full data set (from all seasons) showing that Bogong moths possess a light-dependent magnetic compass. a1-a4.** The orientations of moths (*light blue vectors*) captured during both spring migrations (2023: $\alpha = 231°$, n = 57, $R^* = 1.675$, $p = 6.5\times10^{-3}$, $CI_{95} = 195°\text{-}268°$; 2024: $\alpha = 214°$, n = 65, $R^* = 1.532$, $p = 0.024$, $CI_{95} = 174°\text{-}254°$) and both autumn migrations (2024: $\alpha = 17°$, n = 62, $R^* = 1.179$, $p = 0.048$, $CI_{95} = 319°\text{-}75°$ and 2025: $\alpha = 18°$, n = 64, $R^* = 1.729$, $p = 3.8\times10^{-3}$, $CI_{95} = 342°\text{-}53°$). Moths were flown in a panorama-walled arena and were exposed to a dorsal projection of a full-spectrum randomised starry sky and a natural (0°: *NMF 0*) geomagnetic field (generated by 3-dimensional Helmholtz coils). **b1-b4.** Spring and autumn moths (*light blue vectors*) subjected to the same conditions as in **a1-A4** except with the geomagnetic field (and magnetic north) rotated by 180° (*NMF 180)* (2023 spring: $\alpha = 44°$, n = 62, $R^* = 2.388$, $p = 1.4\times10^{-6}$, $CI_{95} = 19°\text{-}69°$; 2024 spring: $\alpha = 16°$, n = 66, $R^* = 1.916$, $p = 5.0\times10^{-4}$, $CI_{95} = 345°\text{-}47°$; 2024 autumn: $\alpha = 229°$, n = 65, $R^* = 1.58$, $p = 0.016$, $CI_{95} = 190°\text{-}268°$; 2025 autumn: $\alpha = 217°$, n = 67, $R^* = 2.249$, $p = 8.6\times10^{-6}$, $CI_{95} = 191°\text{-}243°$). **c1-c4.** The orientation directions of migratory moths (*light blue vectors*) experiencing a randomised starry sky and a nulled magnetic field during both springs (2023: n = 49, $R^* = 0.471$, $p = 0.524$; 2024: n=73, $R^* = 0.281$, $p = 0.793$) and both autumns (2024: n=65, $R^* = 0.167$, $p = 0.921$; 2025: n=59, $R^* = 0.194$, $p = 0.896$). **d1-d4.** The orientation directions of migratory moths (*orange vectors*) in a natural (0°) geomagnetic field, but this time experiencing randomised stars whose light spectrum had been filtered to exclude UV-blue light (λ >500nm) during both springs (2023: n = 51, $R^* = 0.295$, $p = 0.776$; 2024: n = 55, $R^* = 0.42$, $p = 0.598$) and both autumns (2024: n = 54, $R^* = 0.582$, $p = 0.372$; 2025: n = 61, $R^* = 0.277$, $p = 0.799$). In all panels, each *red mean vector* (*red arrow*) results from weighting the mean directions and mean directedness (vector lengths) of all of the individual moths, as analysed by a one-sided Moore's modified Rayleigh test (MMRT), with Bonferroni correction for multiple comparisons. The direction and directedness of mean vectors is given by α and R^*, respectively. The *dashed circles* show the required R^* value for statistical significance: $p < 0.05$, $p < 0.01$ and $p < 0.001$, respectively for increasing radius. The *shaded areas* show the 95% confidence intervals (CI_{95}). mN, magnetic north.

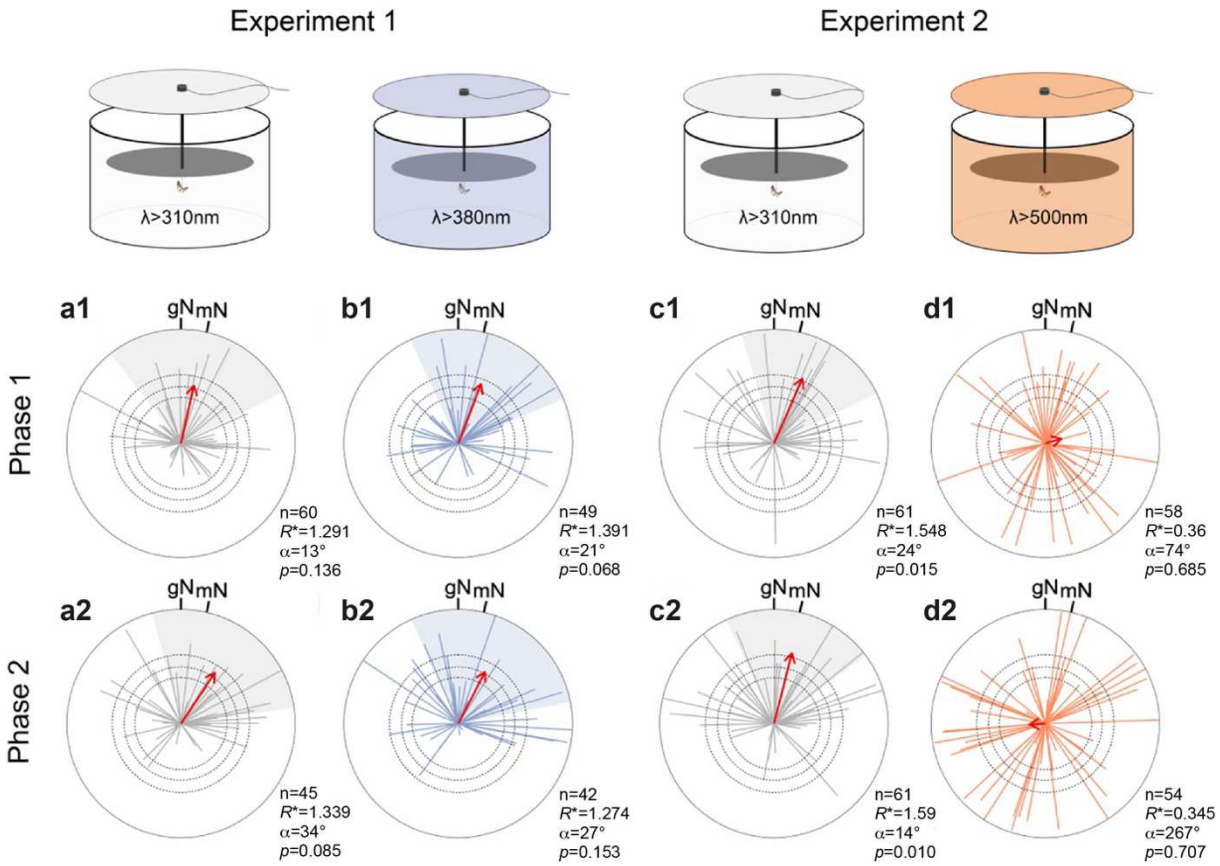
Extended Data Table 1. Watson-Wheeler tests with Bonferroni correction for comparing circular distributions of moth orientation directions across seasons and magnetic field conditions (see Extended Data Fig. 2)

		Watson-Wheeler test		
Group 1	**Group 2**	**W**	***p***	***Corrected p***
2024_Autumn_NMF0	2025_Autumn_NMF0	0.717	0.699	***
2024_Autumn_NMF180	2025_Autumn_NMF180	1.856	0.395	***
2024_Autumn_NULL	2025_Autumn_NULL	0.384	0.825	***
2024_Autumn_NMF0_500nm	2025_Autumn_NMF0_500nm	0.817	0.665	***
2023_Spring_NMF0	2024_Spring_NMF0	1.074	0.585	***
2023_Spring_NMF180	2024_Spring_NMF180	5.298	0.071	***
2023_Autumn_NULL	2024_Autumn_NULL	0.584	0.747	***
2023_Autumn_NMF0_500nm	2024_Autumn_NMF0_500nm	0.259	0.879	***
2024_Autumn_NMF0	2024_Autumn_NMF180	16.989	2.1×10^{-4}	2.5×10^{-3}
2025_Autumn_NMF0	2025_Autumn_NMF180	31.061	1.1×10^{-7}	1.3×10^{-6}
2023_Spring_NMF0	2023_Spring_NMF180	32.647	8.1×10^{-8}	9.7×10^{-7}
2024_Spring_NMF0	2024_Spring_NMF180	31.208	1.7×10^{-7}	2.0×10^{-6}

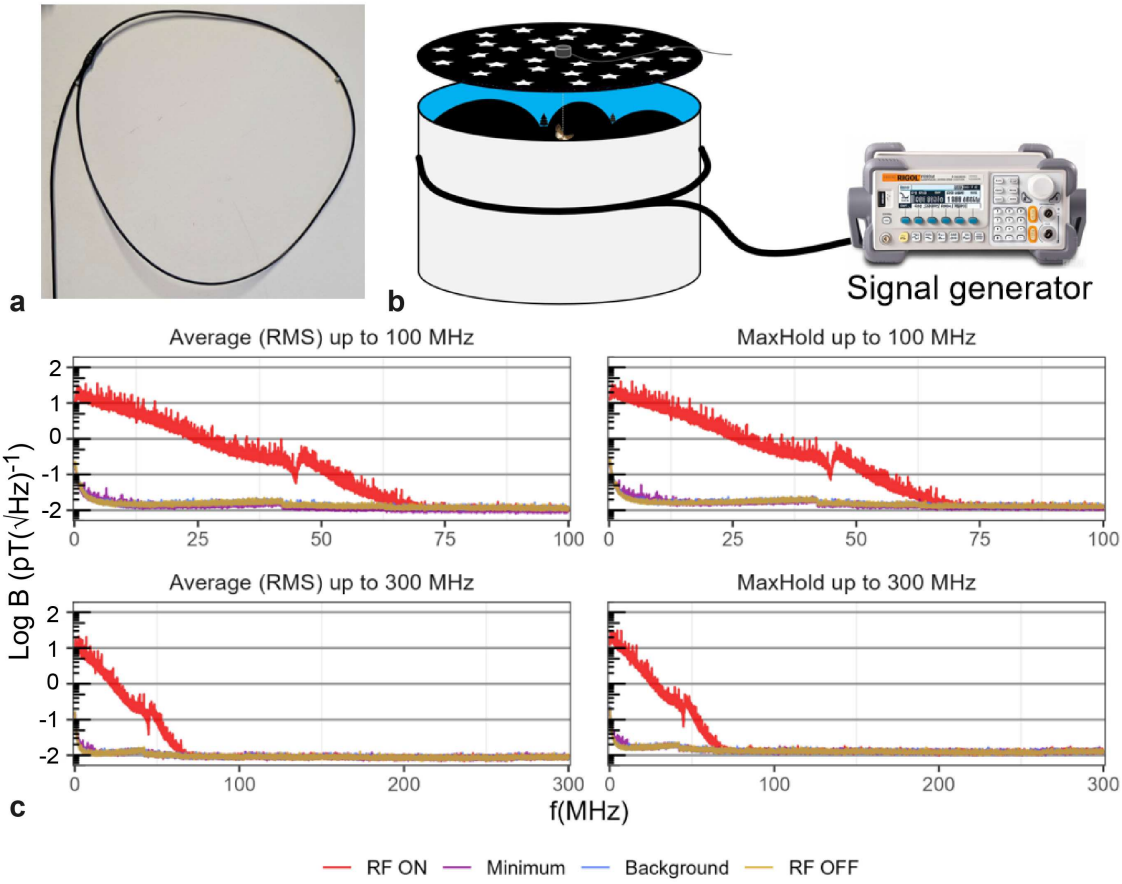
Notes: “500nm” is the illumination spectrum λ>500nm. “NMF0” is a natural geomagnetic field (magnetic north at 0°) and “NMF180” is the natural geomagnetic field rotated by 180° (magnetic north at 180°). “***” means: $p >$ 1



Extended Data Figure 3. **Methods for exploring how the spectrum of illumination influences the geomagnetic compass of migratory Bogong moths. a.** A schematic "map" of the spatial arrangement of two parallel-operated flight simulators controlled from computers located in a black light-tight cubical tent (connecting cables shown as *blue wavy lines*). **b**. Spectral transmission measurements (irradiance) under natural stellar illumination for the four arenas: Clear Arena (1 layer of Lee filter 130, λ > 310 nm), Clear-ND Arena (1 layer of Lee filter 130 and 1 layer of 0.9 ND Lee filter 211, λ > 310 nm), UV-blocking Arena (2 layers of Lee filter 226, λ > 380 nm), and UV-blue-blocking Arena (2 layers of Lee filter 226 and 1 layer of Lee filter 768, λ > 500 nm). The measurement cut-off below Log Irradiance = 5 coincided with measurement noise in the detector (Ocean Optics QE65PRO Spectrometer). **c**. The experimental protocol for exploring the illumination spectral bands required for geomagnetic compass orientation in Bogong moths (in the drawings of the arena, please note the cardboard disk placed on the encoder stalk above the moth to block its view of the night sky, and thus disable its stellar compass). In experiments 1 and 2, two cohorts of ca. 20 moths were flown in parallel in each of two arenas in Phase 1 and then swapped to the other arena in Phase 2 to repeat the experiment. This controlled for the possibility that landscape landmarks seen from within each of the two arenas influenced the orientation of moths (which it did not). In experiment 3, a cohort of ca. 40 moths was flown in an arena with full spectrum illumination ($\lambda > 310$ nm) but reduced in intensity by ca. 8 times by a 0.9 log unit neutral density (ND) filter sheeting. This experiment controlled for the possibility that the intensity-reducing effect of the spectral filtering used in experiments 1 and 2 influenced the orientation of moths (which it did not).



Extended Data Figure 4. The light-dependent magnetic compass of autumn-migratory Bogong moths relies on UV-blue light in both experimental phases (1 and 2) of experiments 1 and 2 (see Main text for details). **a,c.** In a Clear Arena (λ > 310 nm), Bogong moths (*grey vectors*) were oriented in their inherited migratory direction in both phases of experiment 1 (Phase 1, **a1**: $\alpha = 13°$, n=60, $R^* = 1.291$, $p = 0.136$, $CI_{95} = 321°$-63°; Phase 2, **a2**: $\alpha = 34°$, n=45, $R^* = 1.339$, $p = 0.085$, $CI_{95} = 345°$-82°) and in both phases of experiment 2 (Phase 1, **c1**: $\alpha = 24°$, n=61, $R^* = 1.548$, $p = 0.015$, $CI_{95} = 343°$-63°; Phase 2, **c2**: $\alpha = 14°$, n=61, $R^* = 1.59$, $p = 0.010$, $CI_{95} = 335°$-53°). **b.** In a UV-blocking Arena (λ > 380 nm), moths (*light purple vectors*) were also oriented in their inherited migratory direction in both phases of experiment 1 (Phase 1, **b1**: $\alpha = 21°$, n=49, $R^* = 1.391$, $p = 0.068$, $CI_{95} = 335°$-67°; Phase 2, **b2**: $\alpha = 27°$, n=42, $R^* = 1.274$, $p = 0.153$, $CI_{95} = 335°$-79°). **d.** In a UV-blue-blocking Arena (λ > 500 nm), moths (*light orange vectors*) were disoriented in both phases of experiment 2 (Phase 1, **d1**: n=58, $R^* = 0.36$, $p = 0.685$; Phase 2, **d2**: n=54, $R^* = 0.345$, $p = 0.707$). Other Fig. conventions as in Extended Data Fig. 2.



Extended Data Figure 5. **Methods for generating radiofrequency electromagnetic fields to test for a possible disruption of the geomagnetic compass in Bogong moths. a-b.** A photo of an antenna made of coaxial cable. The antenna is placed around the outside wall of the flight simulator arena and connected to a signal and waveform generator (Rigol DG 1022U) via a BNC port. **c**. Measurements of the magnetic components of the RF fields at 2.5 V_{pp} (RF ON - *red*), 0.04 mV_{pp} (Minimum - *magenta*), the generator turned off (Background - *blue*), and the generator in stand-by mode (RF OFF - *yellow*). Average (RMS: root-mean-square; *left column*) and "maxhold" (maximum intensity; *right column*) measurements are shown for the frequency range up to 100 MHz (*top row*) and up to 300 MHz (*bottom row*) to demonstrate the absence of off-target harmonics. The respective density and intensity values are listed in Extended Data Table 3.

Extended Data Table 2. Watson-Wheeler tests with Bonferroni correction were performed to assess differences in directional distributions of moths across experimental phases and light-filtered arena conditions (see Extended Data Fig. 5)

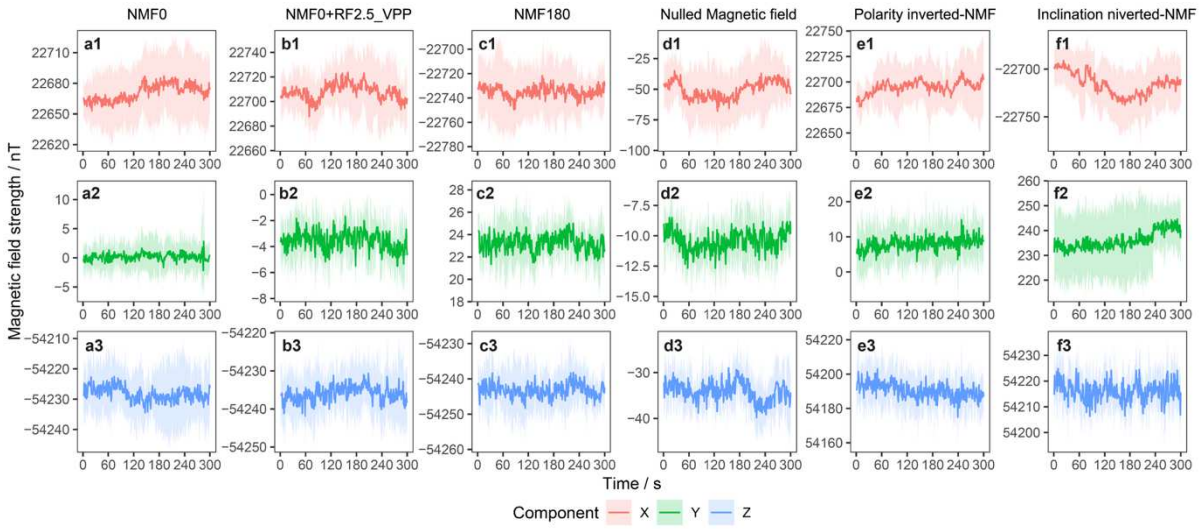
	Watson-Wheeler test				
Experiment	**Group 1**	**Group 2**	**W**	***p***	***Corrected p***
Experiment 1	Clear Arena_Phase1	Clear Arena_Phase2	1.054	0.59	***
	UV-blocking Arena_Phase1	UV-blocking Arena_Phase2	0.412	0.814	***
	Clear Arena_Phase1	UV-blocking Arena_Phase1	0.678	0.712	***
	Clear Arena_Phase2	UV-blocking Arena_Phase2	0.038	0.981	***
Experiment 2	Clear Arena_Phase1	Clear Arena_Phase2	0.263	0.877	***
	UV-blue-blocking Arena_Phase1	UV-blue-blocking Arena_Phase2	0.937	0.626	***
	Clear Arena_Phase1	UV-blue-blocking Arena_Phase1	4.205	0.122	***
	Clear Arena_Phase2	UV-blue-blocking Arena_Phase2	5.243	0.073	***

Notes: “Clear Arena”: illumination spectrum $\lambda > 310$nm. “UV-blocking Arena”: illumination spectrum $\lambda > 380$nm. “UV-blue-blocking Arena”: illumination spectrum $\lambda > 500$nm. “***”: $p > 1$

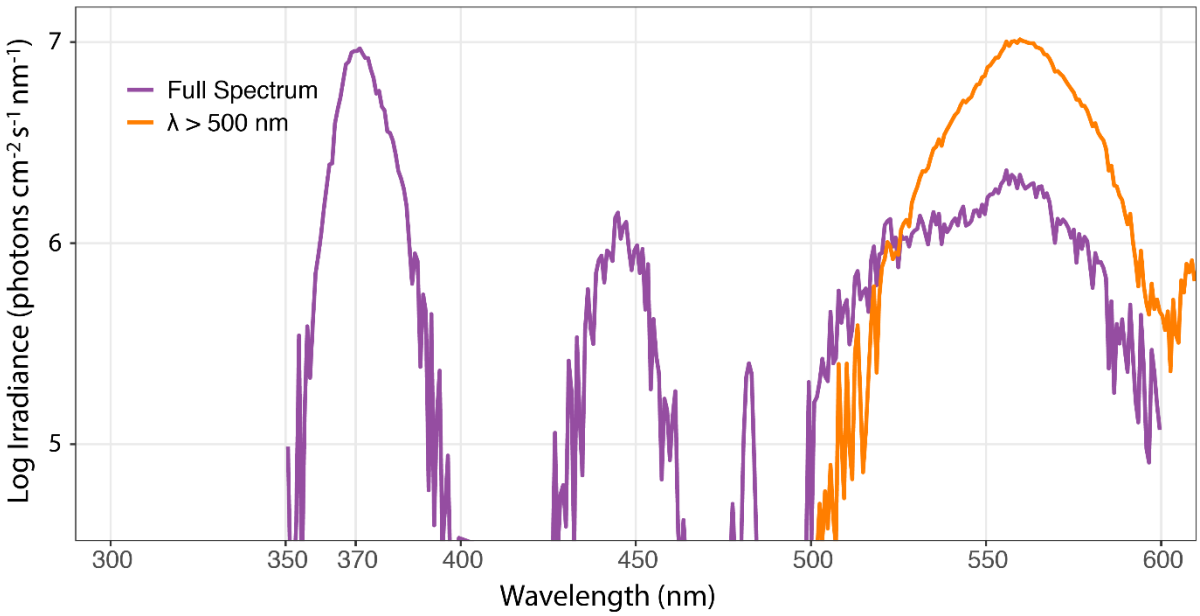
Extended Data Table 3. Noise density and intensity estimates from Reference 13, together with measurements from the present study

Frequency band (kHz)	Species	$\bar{b}^{\max}$ (pT/√Hz)	$\bar{b}$ (pT/√Hz)	B_{rms}^{max} (nT)	B_{rms} (nT)	Effect	Source
10 − 5000	robin	0.07	~0.02	1.18	~0.37	+	Ref. 13 (Fig. 4f, blue trace)
10 − 5000	robin	5.58	~1.8	23.2	~7.35	−	Ref. 13 (Fig. 4f, red trace)
20 − 450	robin	30.1	~9.5	23.1	~7.29	−	Ref. 13 (Fig. 4f, green trace)
600 − 3000	robin	1.35	~0.43	2.3	~0.73	−	Ref. 13 (Fig. 4f, black trace)
150 – 60,000	moth	0.019	0.017	0.178	0.160	+	Present Study (Extended Data Fig. 5c, Background)
110 – 60,000	moth	0.019	0.017	0.180	0.161		Present Study (Extended Data Fig. 5c, RF OFF)
110 – 60,000	moth	0.019	0.015	0.175	0.146		Present Study (Extended Data Fig. 5c, Minimum)
110 – 60,000	moth	3.505	2.877	49.560	40.799	−	Present Study (Extended Data Fig. 5c, RF ON)

Species: *robin* = European robin, *Erithacus rubecula*, *moth* = Bogong moth, *Agrotis infusa*. For calculations of maximum and average density ($\bar{b}^{\max}$, $\bar{b}$), and maximum and average intensity (B_{rms}^{max}, B_{rms}) see Equations (2.1) and (2.3) in Ref. 49. Effect: behavioural experiments resulted in oriented (+) or disoriented (–) animals.



Extended Data Figure 6. The magnetic field conditions used in the laboratory experiments (measured using a Meda FVM-400 magnetometer at the location in the arena where the moth is located). Magnetic fields were generated via a three-dimensional Helmholtz coil system and measured (in nanotesla, nT) six times over 300 s, yielding X, Y, and Z traces. Traces were averaged to compute mean component strengths (X, Y, Z: *red*, *green*, *blue lines*) with standard deviations (*shaded regions*). **a1–a3.** The three-component vector of a natural geomagnetic field (NMF0) at 0° azimuth. **b1–b3.** The three-component vector of NMF0 at 0° azimuth with an imposed 2.5 V_{pp} (volts peak-to-peak) radio frequency (RF) field (NMF0+RF_2.5VPP). **c1–c3.** The three-component vector of a natural geomagnetic field rotated by 180° (NMF180). **d1–d3.** The three-component vector of a nulled geomagnetic field. **e1–e3.** The three-component vector of a natural geomagnetic field with inclination inverted. **f1–f3.** The three-component vector of a natural geomagnetic field with polarity inverted.



Extended Data Figure 7. Measurements of the spectrally filtered stellar illumination used in laboratory experiments. The illumination was provided by the projector (LED projector ASUS S1 Mobile) and a ring of 8 UV-emitting LEDs (LED370E Ultra Bright Deep Violet LED, Thorlabs) centred around the projector's front lens. To manipulate the intensity and spectral composition of light entering the flight arena, we employed filter sheets (Lee Filters, USA) placed in front of the projector lens. For full spectrum illumination (*purple curve*), Neutral Density (ND) filters (Lee Filters 210, ND 0.6 log units and transmitting $\lambda > 310$ nm) were used to attenuate light intensity uniformly across all wavelengths ($\lambda > 310$ nm), preserving spectral integrity. Six layers of Lee Filter 210 were used to reduce illumination levels to natural stellar intensities (*purple curve*). For this spectrum (and during full-spectrum experiments), the ring of UV-emitting LEDS was turned ON). Lee Filter 768 (Egg Yolk Yellow) is a spectral long-pass filter that allows transmission of light from around 500 nm. To block the UV-violet-blue part of the illumination spectrum, and to maintain approximately the same starlight illumination intensity, 1 layer of Egg Yolk Yellow filter (Lee Filter 768, $\lambda > 500$ nm) and 5 layers of 0.6 ND filter (Lee Filters 210) were placed in front of the projector lens (*orange curve*). For this spectrum (and during the $\lambda > 500$ nm experiments), the ring of UV-emitting LEDS was turned OFF). Upward illumination intensity and spectrum measurements of the projected starry night sky were made from within the arena using an Ocean Optics QE65PRO Spectrometer (Ocean Optics) located underneath the projection screen at the position of the moth. The measurement cut-off below Log Irradiance = 5 coincided with measurement noise in the detector.